

portion of the face has been further damaged by surface slides by erosions due to wave actions.

For the above reasons and as required for the purposes of this study, the stability of the dam was analyzed, as described in detail below, by using the currently prevailing methods of analysis.

The analysis was based on the sections of the dam as measured in the field, thus, presenting the current actual conditions. The properties of the embankment materials were as given in the EDCOP-TAMS Report mentioned previously. Certain such values were changed, so different ones were used when considered appropriate.

7.5.2. Data Used in the Analysis

(1) Dam Section

The D-2 Cross Section of the dam shown in Fig. 7.4 was used as a typical section for the stability analysis.

(2) Properties of Embankment Materials

As there are no data on the shear strength of the embankment materials used in the original design, for this analysis, the shear strength was based on preliminary data given in the EDCOP-TAMS Report and the data used for the Ambuklao dam located on the same river not far from Binga. The data used for Binga in this analysis are presented in Table 7.1 below.

The unit weights of the embankment materials for Binga as used in the analysis are shown in Table 7.2, further below. The shear strength tests performed for the core materials of the Ambuklao dam are shown, for comparison, in Table 7.3.

Table 7.1

Shear Strength of the Binga Dam Embankment Materials
as Used for the Stability Analysis

<u>Zone</u>	<u>Internal Friction Angle</u>	<u>Cohesion</u>
Rockfill materials	43°	0
Filter materials	35°	0
Core materials	23°	0.6 kg/cm ²

Table 7.2

Unit Weight of the Binga Dam Embankment
Materials as Used for the Stability Analysis

<u>Zone</u>	γ_d *1	γ_t *2	γ_{sat} *3
Rockfill materials	1.9	2.0	2.1
Filter materials	1.9	2.0	2.1
Core materials	1.8	1.9	2.0

Note: *1 ; Dry condition

*2 ; Wet condition

*3 ; Saturated condition

Table 7.3

Results of the Shear Strength Tests on the Core
Materials of the Ambuklao Dam

- CU Test

Ccu : 0.86 kg/cm², 0.33 kg/cm², 0.71 kg/cm²
φcu : 26° , 26° , 23°

- CD Test

Ccd : 0.66 kg/cm², 0.12 kg/cm², 0.33 kg/cm²
φcd : 28° , 31° , 28°

- Average Value

Ccu : 0.645 kg/cm², Ccd : 0.377 kg/cm²
φcu : 25° , φcu : 29°

Note: Cu ... consolidated and undrained condition
cd ... consolidated and drained condition

(3) Loading Conditions

The following three reservoir water levels were considered in the analysis:

Case 1	F.W.L.	EL.579.5 m
Case 2	N.W.L.	EL.575.0 m
Case 3	L.W.L.	EL.555.0 m

The analysis for Case 3 with the reservoir level at EL.555 m. (L.W.L.), was carried out on the assumption that the water pressure in the core would remain unchanged from that used for the normal reservoir level (N.W.L.), in view of an abrupt drawdown of the reservoir water level.

The Binga dam is located in an earthquake zone. Since the

earthquake affects, to a great extent, the stability of the dam, due consideration should be given in the Study to the seismic conditions occurring in the region. As the design criteria for the earthquake effects used in the original design of the Binga dam are not known due to lack of available data, it was decided to use, instead, the seismic conditions used for the Ambuklao dam. A seismic coefficient is set as $kh = 0.15$.

7.5.3. Method of the Analysis

The dam stability analysis was carried out by the Slice Method using a circular sliding surface.

The particulars of this method are as follows:

Slice Method Using a Circular Sliding Surface

$$n = \frac{\sum \{C + (N - U - N_i) \tan \phi\}}{\sum (T + T_i)}$$

where,

N : Vertical component of force acting on a sliding surface of each slice

T : Tangent component of force acting on a sliding surface of each slice

U : Pore pressure acting on a sliding surface of each slice

N_i : Vertical component of inertia force acting on a sliding surface of each slice at the earthquake

T_i : Tangent component of inertia force acting on a sliding surface of each slice at the earthquake

ϕ : Internal friction angle of materials on a sliding surface of each slice

C : Cohesion of materials on a sliding surface of each slice

l : Length of a sliding surface of each slice

Then, N , T , N_i , T_i , U are expressed as below :

The following signs used in formulas denote :

γ_w : Unit weight of water

γ_i : Wet unit weight

γ_{sat} : Saturated unit weight

γ_{sub} : Submerged unit weight

k : Seismic coefficient of the dam

u : Pore pressure per unit length

1) Non-loaded

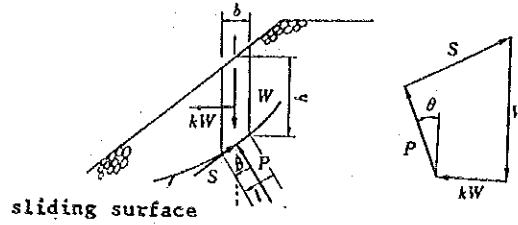
$$N = W \cos \theta = bh \gamma_i \cos \theta$$

$$Ne = W k \sin \theta = kbh \gamma_i \sin \theta$$

$$U = ul$$

$$T = W \sin \theta = bh \gamma_i \sin \theta$$

$$Te = kW \cos \theta = kbh \gamma_i \cos \theta$$



Components of force by Slice Method (Non-loaded)

2) Full water level (Static water pressure added)

$$N = W \cos \theta + \Delta E \sin \theta$$

$$= (W_1 + W_w) \cos \theta + (E_n - E_{n+1}) \sin \theta$$

$$= (\gamma_{sat} h_1 + \gamma_w h_w) b \cos \theta + \gamma_w h b \sin^2 \theta / \cos \theta$$

$$= \gamma_{sat} h_1 b \cos \theta + \gamma_w h b / \cos \theta$$

$$Ne = W_1 k \sin \theta + (E_n - E_{n+1}) \cos \theta$$

$$= k \gamma_{sat} h_1 \sin \theta + (E_n - E_{n+1}) \cos \theta$$

$$U = ul = \gamma_w h b / \cos \theta$$

$$T = W \sin \theta - \Delta E \cos \theta$$

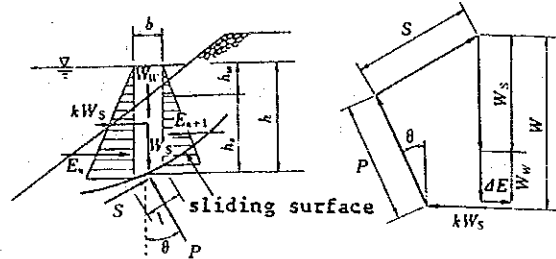
$$= (W_1 + W_w) \sin \theta - (E_n - E_{n+1}) \cos \theta$$

$$= (h_1 \gamma_{sat} + h_w \gamma_w) b \sin \theta - \gamma_w h b \sin \theta$$

$$= bh_1 \gamma_{sat} \sin \theta$$

$$Te = kW_1 \cos \theta$$

$$= kh_1 \gamma_{sat} \cos \theta$$



Components of force by Slice Method (Full water level)

3) Partial stored - water (Static water pressure added)

$$N = W \cos \theta +$$

$$\Delta E \sin \theta$$

$$= (W_1 + W_2) \cos \theta$$

$$+ (E_n - E_{n+1})$$

$$\sin \theta$$

$$= (\gamma_1 h_1 + \gamma_{sat} h_2)$$

$$b \cos \theta + (E_n -$$

$$E_{n+1}) \sin \theta$$

$$Ne = (W_1 + W_2) k \sin \theta + (E_n - E_{n+1}) \cos \theta$$

$$= (h_1 \gamma_1 + h_2 \gamma_{sat})$$

$$k b \sin \theta + (E_n - E_{n+1}) \cos \theta$$

$$U = ul$$

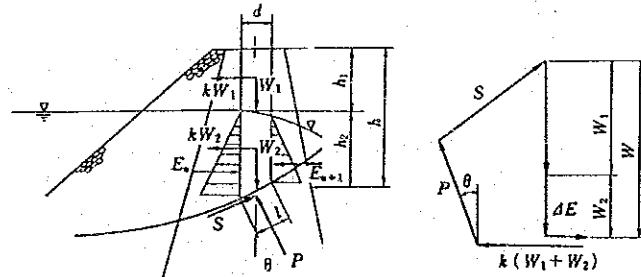
$$T = W \sin \theta - \Delta E \cos \theta$$

$$= (W_1 + W_2) \sin \theta - (E_n - E_{n+1}) \cos \theta$$

$$= (h_1 \gamma_1 + h_2 \gamma_{sat}) b \sin \theta - (E_n - E_{n+1}) \cos \theta$$

$$Te = (W_1 + W_2) k \cos \theta$$

$$= (h_1 \gamma_1 + h_2 \gamma_{sat}) k \cos \theta$$



Components of force by Slice Method (Partial stored - water)

7.5.4. Results of the Analysis

(1) Stability Analysis of the Upstream Slope

The stability analysis of the upstream slope of the dam is normally carried out on various conditions, such as immediately after completion of the embankment, for full reservoir water level and an abrupt reservoir drawdown with or without seismic loading. Six various cases were analyzed by combining the above loading conditions. Flood, normal and low reservoir operating conditions were considered. Each of these conditions was investigated with and without the earthquake effects included. The results of this analysis are shown in Table 7.4, below.

Table 7.4
Safety Factor against Sliding for
the Upstream Slope

Conditions		Large slides		Small slides	
		Safety factor	Radius of sliding (m)	Safety factor	Radius of sliding (m)
At normal situation (N)	F.W.L.	2.16	92.5	1.25	22.6
	N.W.L.	2.06	117.5	1.26	28.3
	L.W.L.	1.67	103.3	1.32	78.0
At earth-quake (S)	F.W.L.	1.18	110.6	0.81	33.0
	N.W.L.	1.16	110.6	0.87	33.7
	L.W.L.	1.06	98.5	0.98	78.0

Two types of slides by size, termed large and small, were investigated. It is assumed that the small size could appear in the upper portion of the upstream face of the dam only, while the large slides could affect the whole slope. Potential sliding surfaces related to the cases given in Table 7.4 are drawn in Fig.7.5. With a reference to this table and figure, the results of the analysis are evaluated as follows:

For normal loading conditions, all safety factors against sliding for both the large and small slides indicate a value higher than 1.25 at any reservoir water level. Comparison of the safety factors between the large and small slides indicates that the latter is smaller than the former. This is due to the fact that the slope gradient of the upper portion of the dam is as gentle as 1:30. With regard to the reservoir water level conditions, the safety factor against sliding for the large slide at the low water level is found smaller, as the residual water pressure in the core due to the abrupt drawdown of the water level is assumed to be effective.

When the earthquake effects are included, the safety factor against sliding for the large slide is larger than 1.0 (the minimum 1.06) at any water level, but that for the small slide is in a range of 0.81 to 0.87. Consequently, with the present condition of the upper portion of the dam kept as it is, the small slides may be caused on the occasion that an earthquake with a design seismic coefficient $K_h=0.15g$ take place at the full or high water levels. Listed in Table 7.5 below for reference are seismic coefficients which make the safety factor against sliding for the small slides to be 1.0 with the present shape of the dam maintained. Those values are found to be 50% to 90% of the design values.

Table 7.5.

Seismic Coefficients Applied for Stability
of the Dam Upstream Face

Reservoir Water Level	Seismic Coefficient Applied for Safety Factor 1.0	Radius for Sliding (m)	Return Period (Year)
F.W.L.	0.075	30.79	79
H.W.L.	0.090	32.61	115
L.W.L.	0.135	72.79	301

(2) Stability Analysis of the Downstream Slope

Six different cases were also investigated in the stability analysis of the downstream slope. Here, again, the three different water levels in the reservoir, flood, normal and low, were considered. Each case was investigated with and without the earthquake. For all cases investigated, the safety factor was found to be above 1.0. Large and small slides, as was the case for the upstream slope, were also investigated. The results of the analysis are shown in Table 7.6.

It is also found for the downstream slope that the safety factor of the smaller slides is lower than that of the larger slides.

This is again attributable to the fact that the slope gradient of the upper portion of the dam is steep. Both small and large slides indicate safety factors higher than 1.5 for normal loading conditions. For cases when the earthquake is included, the safety factor for small slides on the downstream slope is no less than 1.15.

Table 7.6.

Safety Factor against Sliding on
the Downstream Slope

Conditions	Large slides		Small slides		
	Safety factor	Radius of sliding (m)	Safety factor	Radius of sliding (m)	
At normal situation (N)	F.W.L.	1.71	724.3	1.55	40.45
	N.W.L.	"	"	"	"
	L.W.L.	"	"	"	"
At earthquake (S)	F.W.L.	1.23	1,529.6	1.15	"
	N.W.L.	"	"	"	"
	L.W.L.	"	"	"	"

7.5.5. Recommendations and Conclusions

In accordance with the results of the stability analysis of the dam described above, it is found that the earthquake effects could cause problems with the stability of the upstream slope of the dam. This is attributable to the slope gradient of the upper portion of the dam which at certain locations of this portion is as steep as 1:1.30. It is, therefore, proposed in the rehabilitation plan to rebuild this portions of the dam by backfilling and provide a slope with a uniform gradient of no less than 1:2.23. The cross section of the repaired slope is shown in Fig.7.6.

Stability analysis of the new (repaired) section of the dam was carried out using the same assumptions, loading conditions, and principles as shown above. The results of the analysis are shown in Table 7.7 and Fig.7.7. The safety factors for normal operating conditions are all well above 1.0, with the minimum equal to 1.50. The minimum safety factor with the earthquake included is 1.0.

It is also noticed that as compared with the existing dam section, the safety factors against sliding of the repaired section are smaller for the case of large slides. The reason for this is the increased mass of the dam due to the new backfill materials added which increase the size of the sliding force.

Table 7.7.
Safety Factors for the Upstream Slope after Repairs

Conditions	Large slide		Small slide		
	Safety factor	Radius of sliding (m)	Safety factor	Radius of sliding (m)	
At normal situation (N)	F.W.L.	1.92	98.8	2.01	49.2
	N.W.L.	1.84	106.6	2.04	44.3
	L.W.L.	1.50	106.6	2.16	95.4
At earth-quake (S)	F.W.L.	1.09	118.2	1.23	49.24
	N.W.L.	1.09	118.2	1.37	40.3
	L.W.L.	1.00	106.6	1.50	189.1

7.6. Probability of Earthquake at Binga Site

7.6.1. Record of Earthquakes

The return period of the earthquake at Binga site located at 16.395 degrees of north latitude and 120.728 degrees of east longitude was studied using the records of earthquakes covering the area of 13 to 19 degrees of north latitude and 119 to 123 degrees of each longitude. (Extracted from "Earthquake Listing, Area: Latitude 13-19 degrees, Longitude 119-123 degrees, Source: Preliminary Determination of Epicenter - Monthly listing, U.S. Department of the Interior/Geological Survey National Earthquake Information" and other sources).

The above sources of information cover a period of 91 years from 1896 to 1986 out of which 54 years are available with the relevant data provided as required. There occurred the earthquakes 1,550 times during this period, and the dates and time of occurrence, locations of epicenters (latitude/longitude), depths of hypocenters and the magnitudes are recorded therein.

7.6.2. Probability of Earthquake

In respect of the abovementioned all earthquakes, the equivalent seismic forces at Binga site were obtained using the Kanai formula which is expressed as below:

$$\log a = 0.61 M - \left(1.66 + \frac{3.60}{X}\right) \log X + \left(0.167 - \frac{1.83}{X}\right) + 100 \frac{1}{T}$$

a : gal. acceleration (cm/sec.²)

X : distance from hypocenter (km)

M : magnitude

T : predominant period (sec.)

The predominant period is a function of the distance from an hypocenter (X) and the magnitude (M) as illustrated in Fig.7.8.

Subsequently, the maximum seismic force at each year a was checked with its probability $\phi(a)$ using the Gumbel III distribution function which is expressed as below:

$$\phi(a) = \exp. \left\{ - \left(\frac{\ln W - \ln a}{\ln W - \ln v} \right)^k \right\}$$

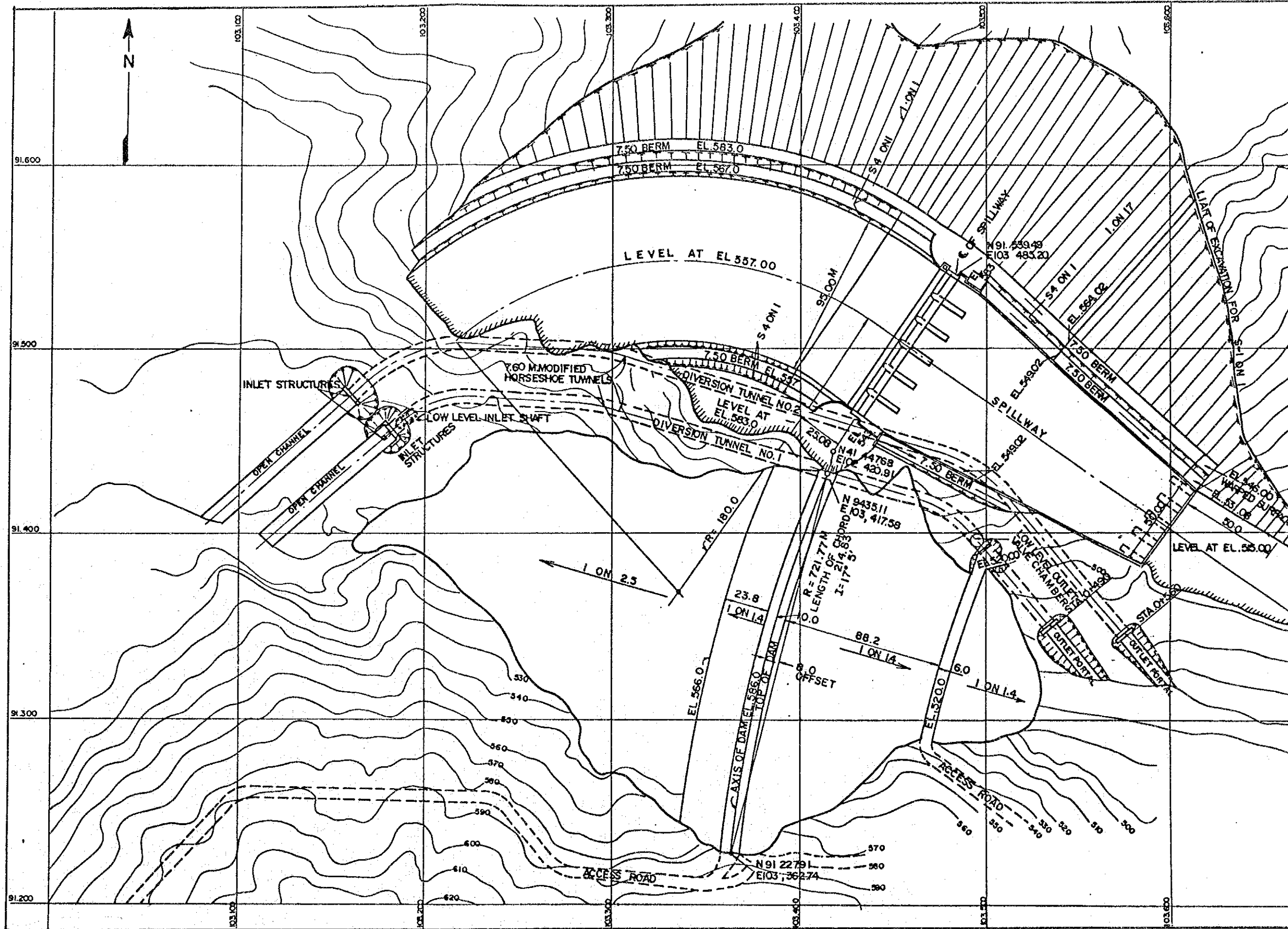
where, W , v and k are parameters to fix a form of distribution, which are determined by the method of least squares so as to suit the actual form of distribution. After this distribution function has been determined, a return period T (year) can be obtained from the relation of $T = 1/(1-\phi(a))$. As the result of calculations, the parameters of the distribution function for the Binga site indicated the following values:

$$W = 578.965, v = 1.210, k = 3.988$$

Fig.7.9 shows the data used for the calculations and the distribution curve led by the procedures abovementioned.

Further, the seismic force a (gal) corresponding to the return period T year is obtained from the above distribution curve as shown in the following table, in which the seismic force $kh=0.15g$ (=147 gal) used before for the study on the dam stability is found to correspond to an earthquake of the 400-year return period.

<u>Return Period and Seismic Force</u>						
Return Period (year)	5	20	50	100	200	400
Seismic Force (gal)	8	31	57	83	113	147



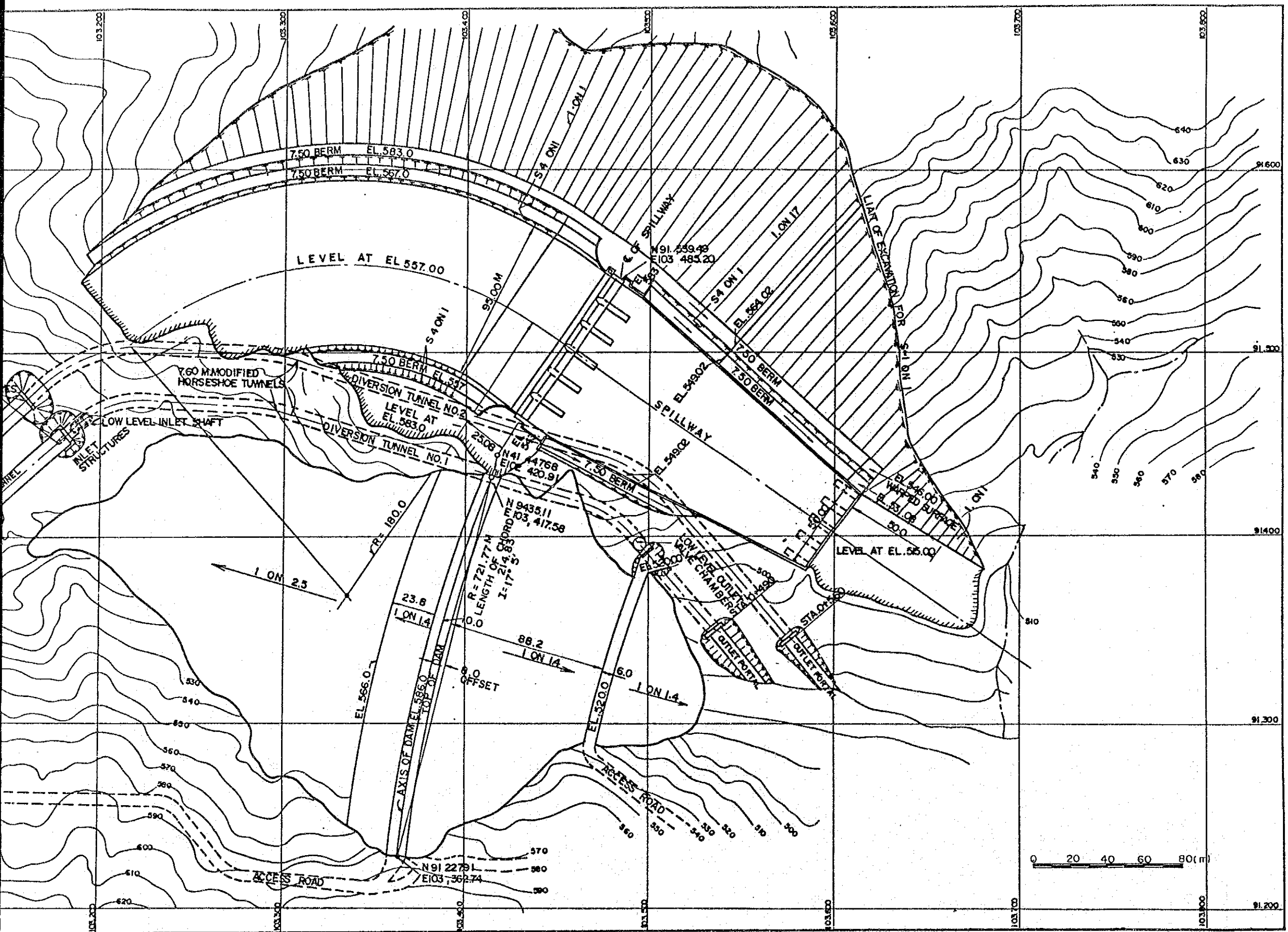


Fig. 7.1

THE BINGA DAM REHABILITATION PROJECT	
General Layout of Dam and Spillway	
SCALE	DATE
THE JAPAN INTERNATIONAL COOPERATION AGENCY	

DAM TYPICAL CROSS SECTION (DESIGN)

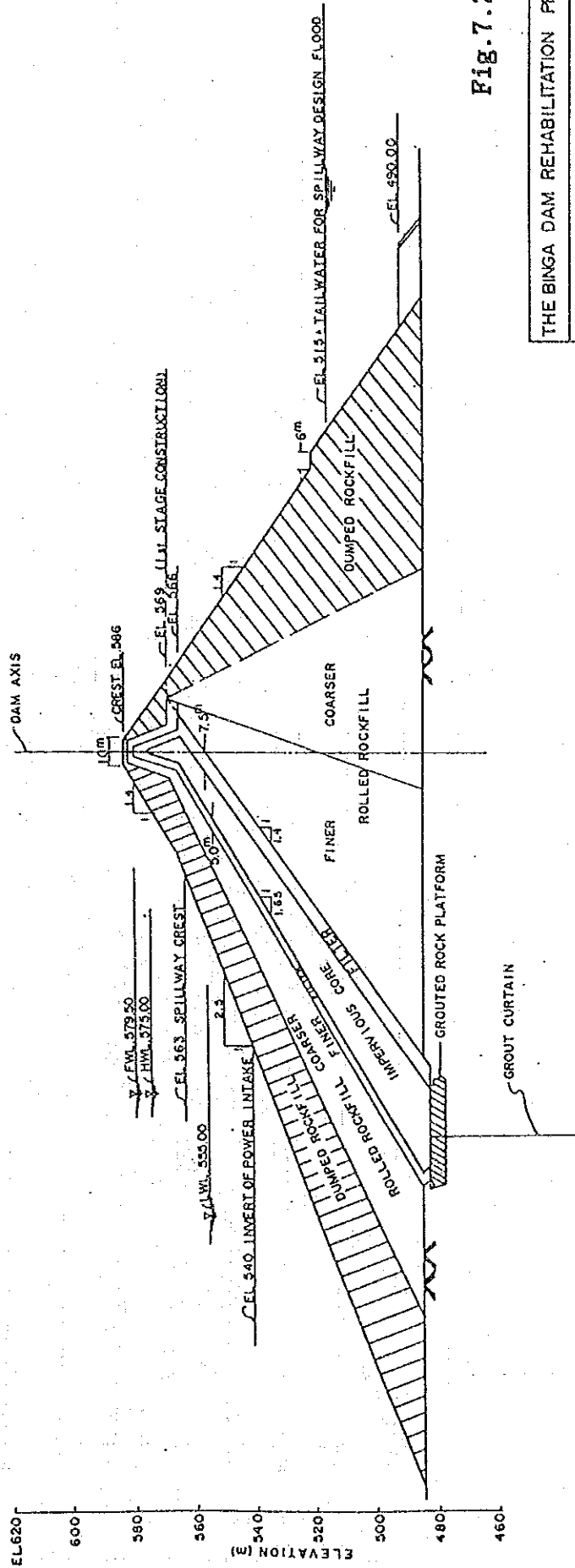


Fig. 7.2

THE BINGA DAM REHABILITATION PROJECT	
Typical Cross Section of the Dam (Designed)	
SCALE	DATE
THE JAPAN INTERNATIONAL COOPERATION AGENCY	

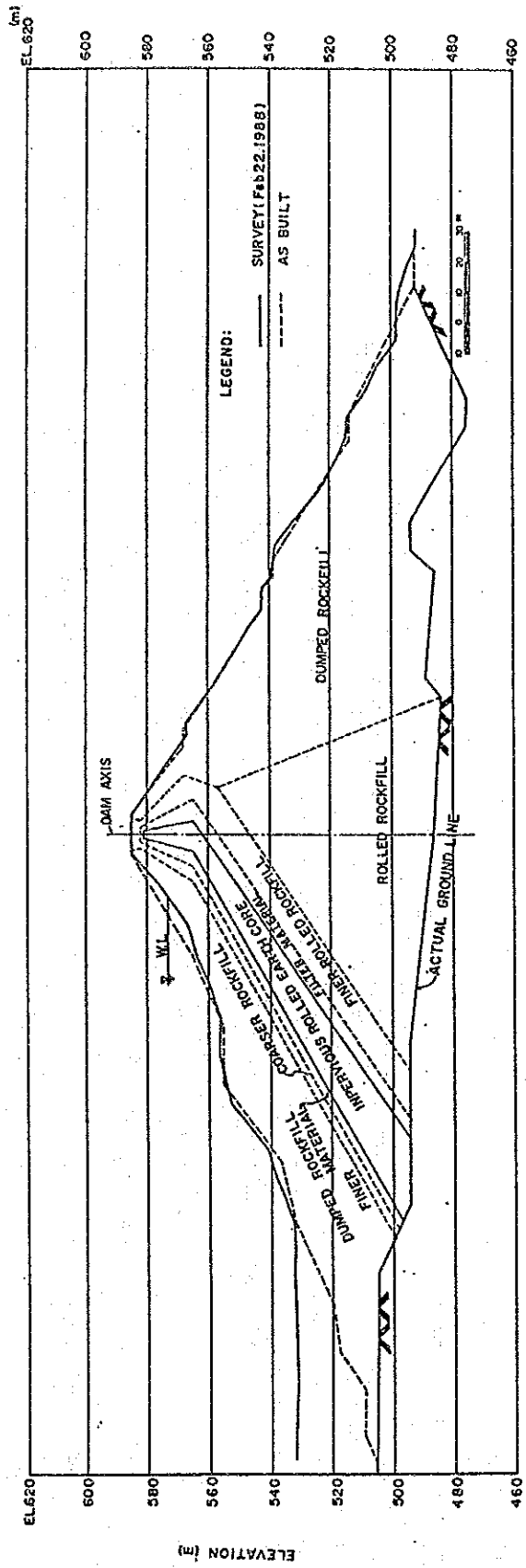


Fig. 7.3

THE SINGA DAM REHABILITATION PROJECT	
Cross Section of Dam	
As Built and As Surveyed	
SCALE	DATE
THE JAPAN INTERNATIONAL COOPERATION AGENCY	

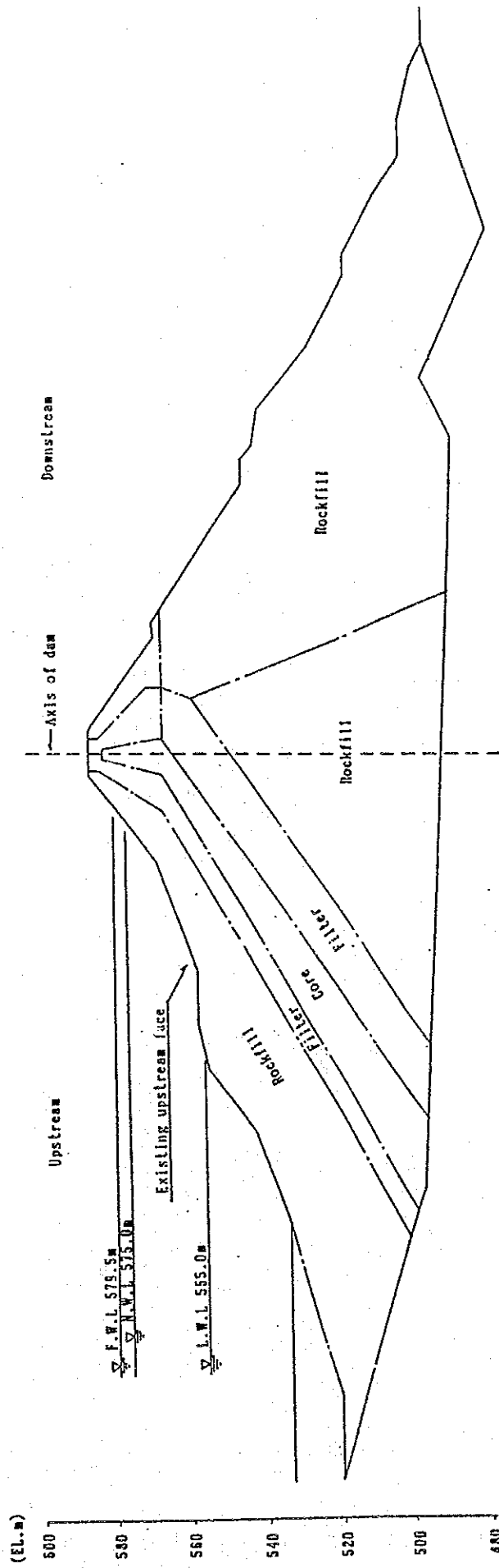


Fig. 7.4 Binga Dam Cross Section D2 Typical Section As Surveyed in 1988

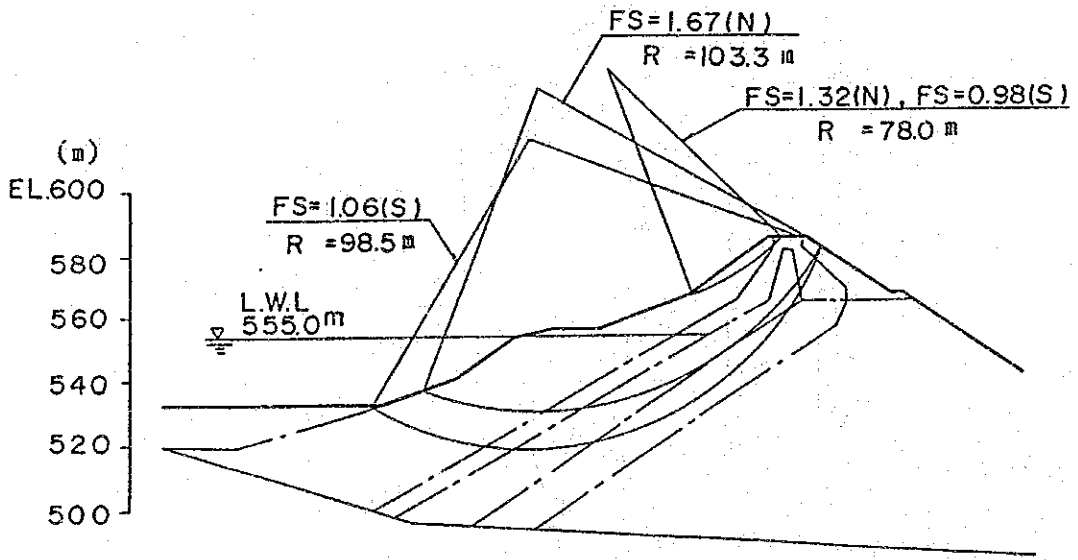
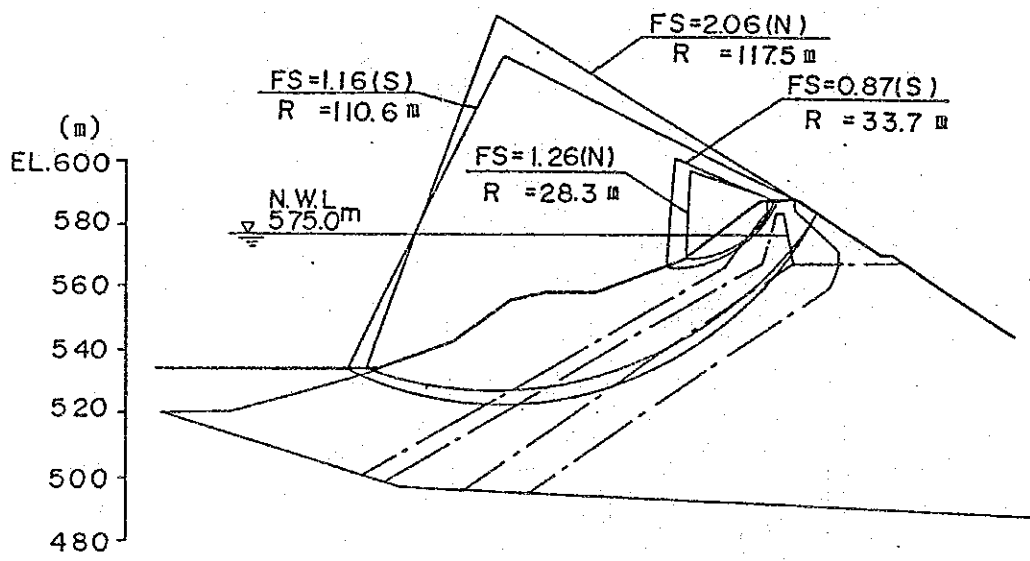
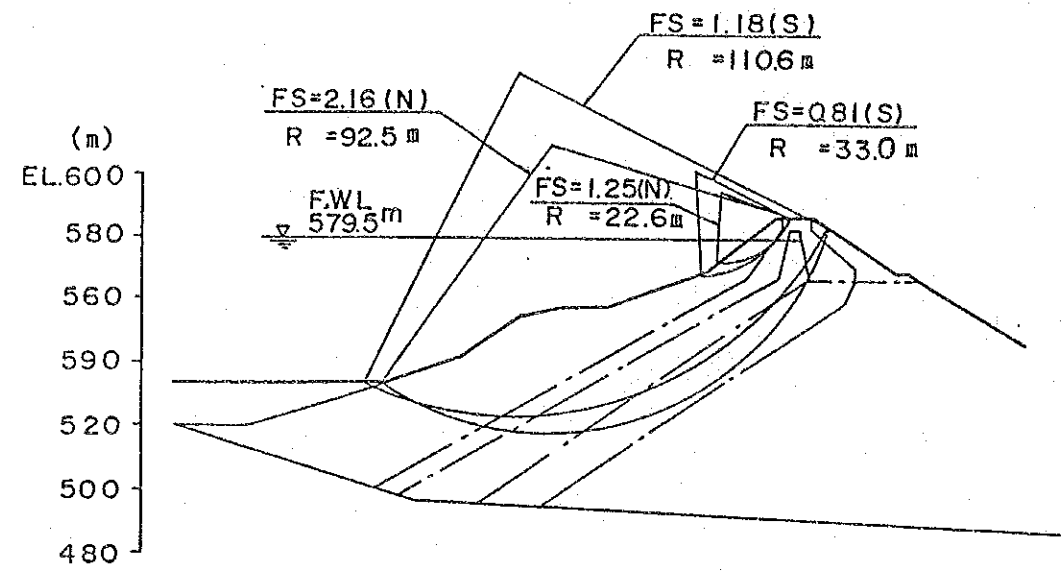


Fig. 7.5 Potential Sliding Surfaces and Safety Factors

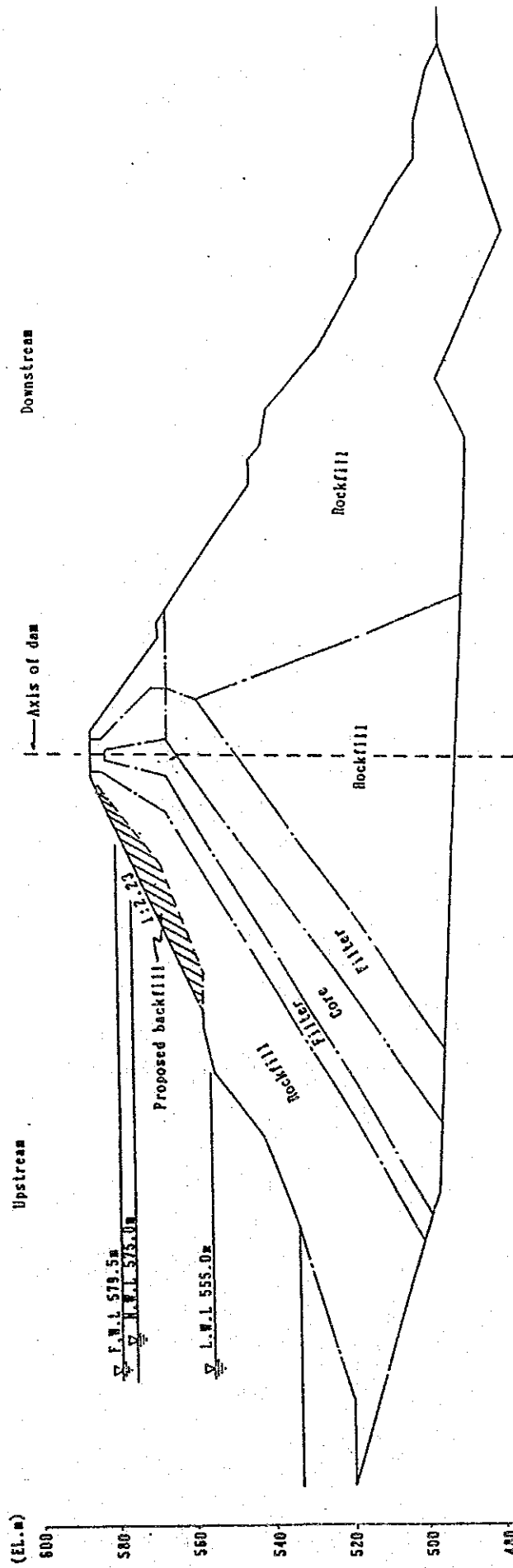


Fig. 7.6 Binga Dam Cross Section D2 Proposed Rehabilitation Measures

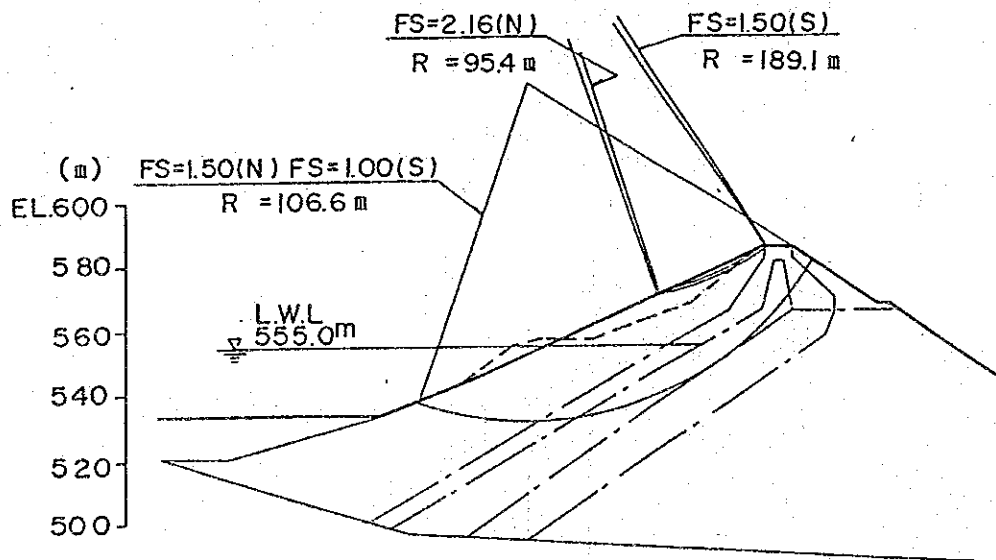
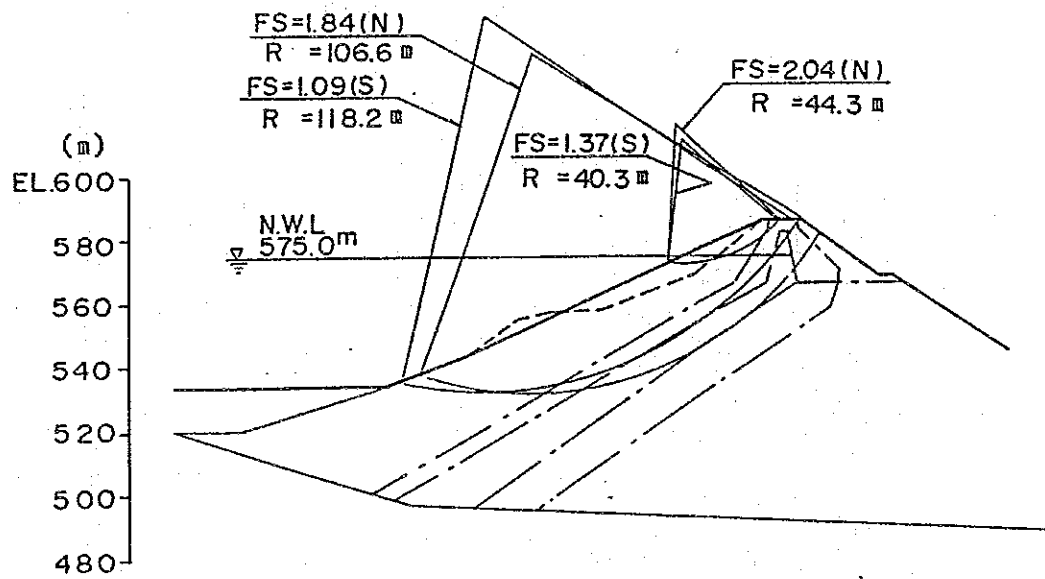
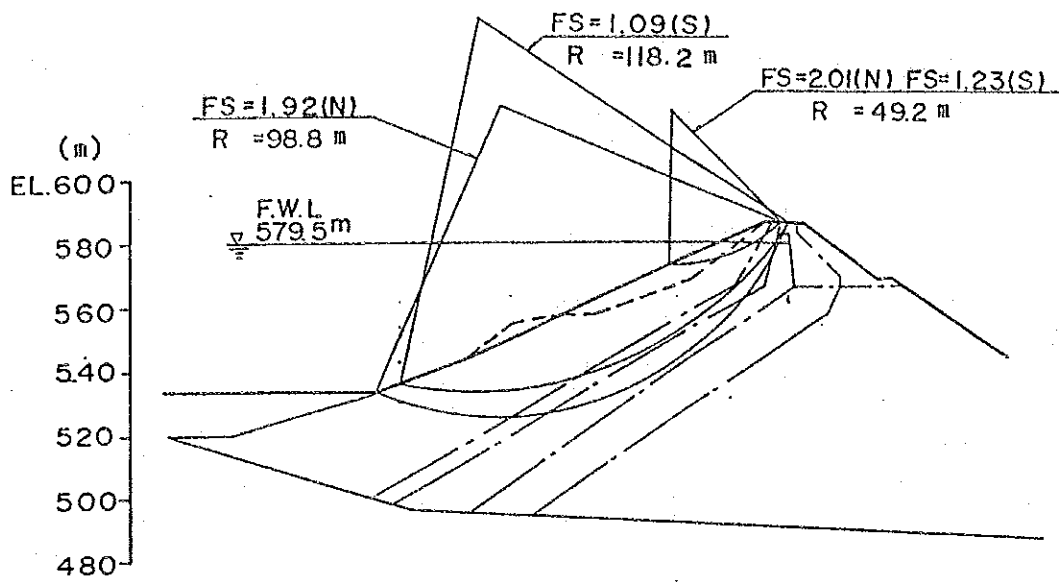


Fig. 7.7 Potential Sliding Surfaces and Safety Factors
(After Rehabilitation)

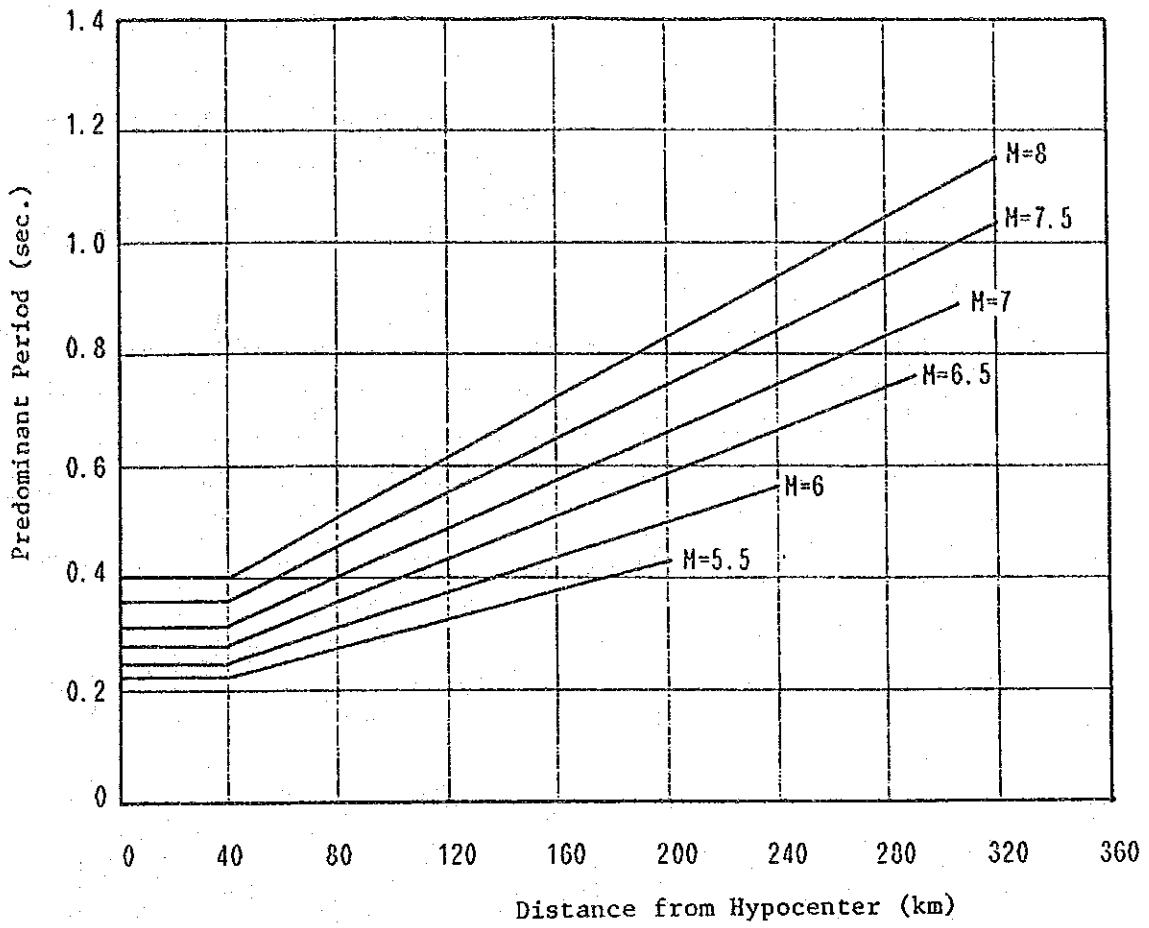


Fig.7.8 Predominant Period of Maximum Acceleration in Rock

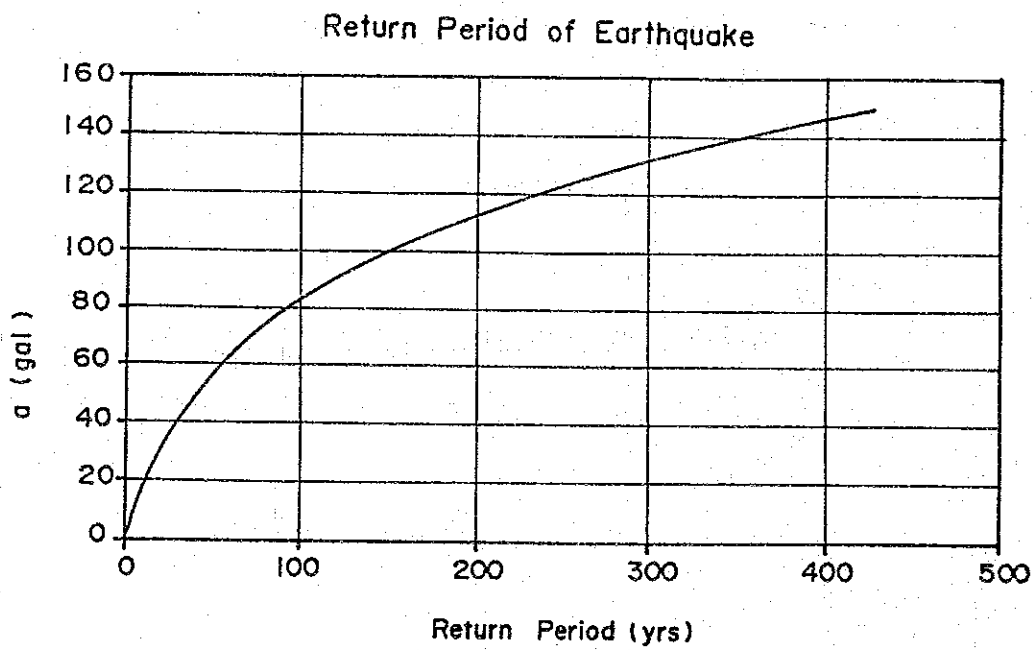
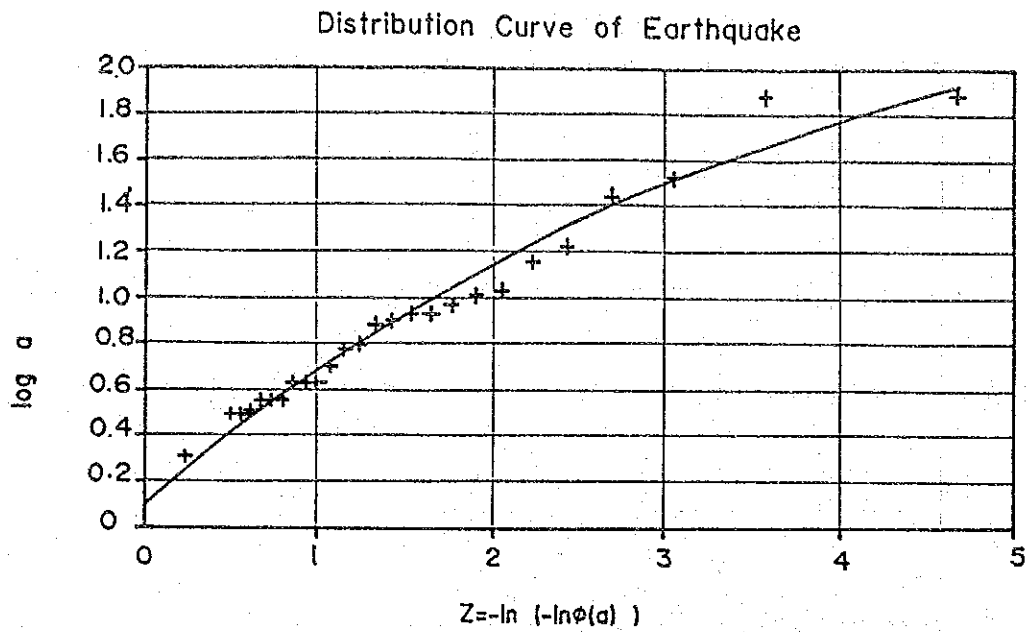


Fig. 7.9 Return Period of Earthquake

8. LEFT BANK OPEN-CUT EXCAVATION

8. Left Bank Open-cut Excavation

8.1. General

The left bank spillway open-cut excavation slope is 130 meters high and about 500 meters long. The geologic features of the slope are shown in Figs. 6.2 through 6.5. Most rocks comprising the slope belong to CM class with some distributions of CL and D classes of rock in the upper portions of the slope. In addition, few faults are observed in the CM class rocks.

In this section, the stability analysis was carried out for all possible slides all over the slope on the assumption that rocks of each class are uniform in properties. Local sliding due to the fractured zone such as faults was studied somewhere in Section 6 "Geology".

8.2. Stability Analysis of the Excavated Slope

8.2.1. Sections Considered in the Analysis

Of all the sections of the slope surveyed currently, Section S-2 was chosen for the analysis because it contained the thickest layers of CL and D class rocks in question. Section S-2 is exhibited in Fig.8.1.

8.2.2. Assumptions

As currently there are no data on the shear strength of the rocks constituting the slope, assumed values have been recommended by the geologists as shown in Table 6.2, in which unit weight values used in the analysis are also given. The ground water level was assumed to be at the ground surface level, taking into account the extremely high rainfall intensity. The seismic coefficient k_h was assumed 0.15, the same as that applied to the dam stability analysis.

8.2.3. Methodology

The method used in the stability analysis of the left bank excavated slope was the Slice Method based on a circular sliding surface. This was the same method as that used for the stability analysis of the dam.

Based on the following procedures, the possible slides were assumed and the minimum safety factor against sliding was obtained.

- (1) To set node points on the profile of the slope every three to four meters in the horizontal direction as shown in Fig.8.1. The berm portions at which gradients of the slope change are set as node points.
- (2) To assume starting points of sliding on the top portion of the slope; EL.740 m, Node Nos. 69 to 80, and then to select, as ending points of sliding, those points at which gradients of the slope change, for the purpose of checking the stability of the whole slope.
- (3) To assume each point of the slope at which the gradient changes as a starting point or an ending point of sliding, for the purpose of checking the stability of each berm.
- (4) To assume sliding surfaces with the starting and ending points of sliding moved in a range of the adjacent five to six nodes for both cases of (2) and (3) above.
- (5) To search the minimum safety factor against sliding by changing a radius of the sliding circular arc one after another for all assumed sliding surfaces.

8.3. Results of the Analysis

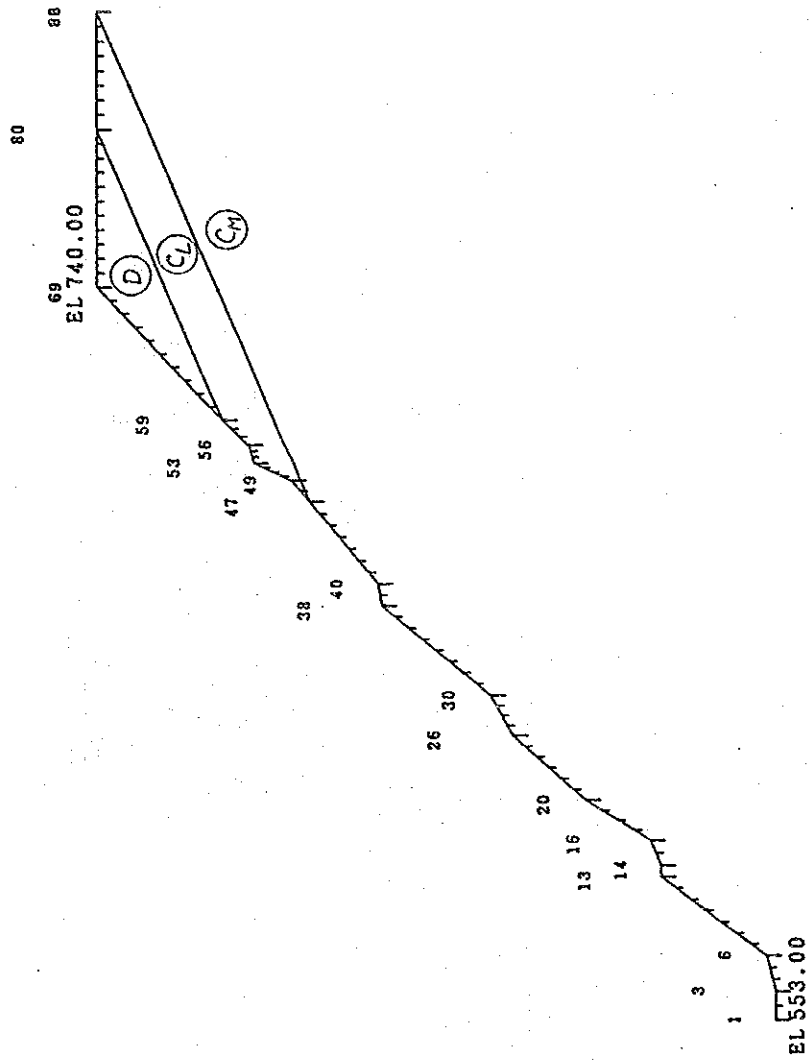
As the results of the analysis for possible slides on the left bank excavated slope, it was found the sliding surface which indicated the smallest safety factor against sliding passes through the D class rocks in the top portion of the slope. The safety factor (F_s) in this case shows 2.87 at the normal condition and 2.30 at the earthquake, which fact can ensure the safety of the slope against sliding. (Refer to Fig.8.2)

Shown in Table 8.1 is a summary of the results of the analysis for possible sliding surfaces mentioned in the preceding sub-section. According to this table, it is revealed that the safety factors against sliding are 9.1 to 13.5 with regard to the sliding surface between each berm of the slope, and 3.1 to 6.6 with regard to the sliding surface between the top portion of the slope and respective berms.

Table 8.1

Stability Analysis of the Left Bank Excavated Slope

Elevation of Starting Point of Sliding		Assumed Sliding Surface				Normal Condition			Earthquake
EL.(m)	Elevation of Ending Point of Sliding	Height of the Slope	Starting Node No.	Ending Node No.	Radius of Sliding Circular Arc	Safety Factor	Safety Factor	Safety Factor	
EL.(m)	EL.(m)	(m)	No.	No.	(m)				
740	716	24	73	62	67.8	2.87	2.87	2.30	
740	687	53	73	49	108.9	4.47	4.47	3.67	
740	662.5	77.5	74	39	84.9	6.63	6.63	5.48	
740	626	114	72	26	95.6	4.82	4.82	3.98	
740	585	155	72	14	128.6	3.67	3.67	3.04	
740	553	187	72	3	154.9	3.14	3.14	2.60	
699	663	36	56	40	27.8	13.47	13.47	11.34	
665.7	626	39.7	41	26	31.5	11.37	11.37	9.72	
632	585	47	30	14	35.7	9.10	9.10	7.86	
586.5	555.5	31	15	6	22.6	12.67	12.67	11.05	



***** LEFT BANK *****

Fig. 8.1 Sections Used for Stability Analysis

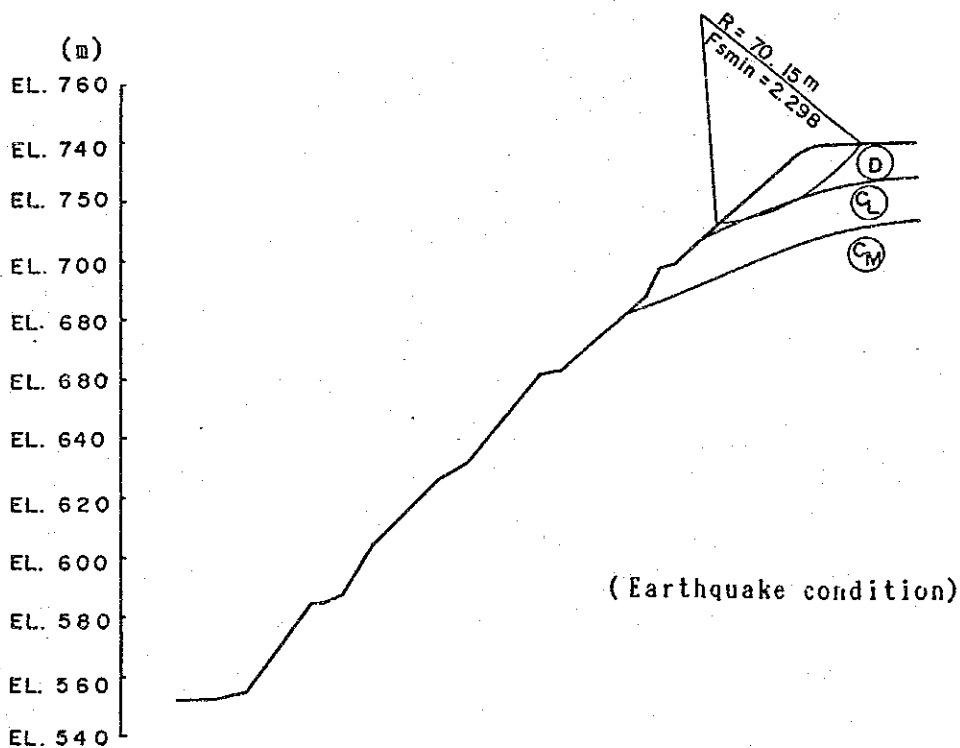
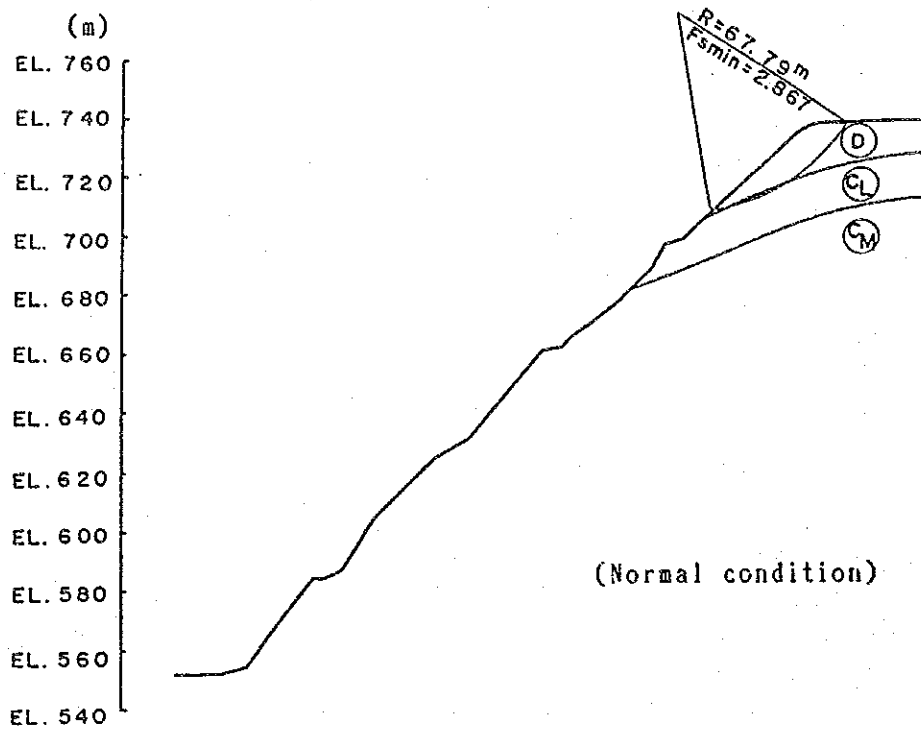


Fig. 8.2 Potential Sliding Surfaces and Safety Factors

9. SPILLWAY AND PLUNGE POOL

9. Spillway and Plunge Pool

9.1. Hydrologic Analysis

9.1.1. Agno River and Binga Dam Basin

The Agno River originates from a high rainfall area in the central region of the Luzon Island, with annual average rainfall of about 3,000 mm, which can be ranked as one of the highest in the world. The river extends for about 300 km in length and reaches the sea at the Lingayen Gulf, as shown in Fig.9.1.

The Binga dam, completed in 1959, is located in the mid stream of the river and has a combined drainage area of 936 km². The dam is of rockfill construction and is designed for the single purpose of generation of electricity. Located some 13 km upstream of the dam as shown in Fig.9.3 is the Ambuklao dam, which was completed in 1956, and has a combined drainage area of 690 km². The Binga dam basin excluding Ambuklao dam basin has a drainage area of 246 km².

The principal tributaries of the Agno River flowing into the Binga reservoir are Besal, Adonot and Sadyo with a drainage area of 147 km², 69 km² and 2.5 km², respectively, as shown in Fig.9.4. These tributaries flow into the reservoir at locations some 11, 5.5 and 0.9 km upstream of the damsite, respectively.

9.1.2. Location of Hydrologic Observation Stations and Observation Periods

The location of the hydrologic observation stations of the Binga dam basin and the neighboring areas is as shown in Fig.9.3.

The observation period by station is shown in Table 9.1.

9.1.3. Records on Rainfall

(1) Correlation of Monthly Rainfall between Observation Stations

Shown below is the monthly and annual average rainfall at the Binga damsite obtained from the data taken over the 31-year period from 1957 to 1987:

Monthly Average Rainfall:

January	6.1 mm
February	5.0
March	37.5
April	68.3
May	271.4
June	345.7
July	530.6
August	508.9
September	344.7
October	204.3
November	82.0
December	13.4

Annual Average Rainfall: 2,417.9 mm

As can be seen from the above, the rainy season for each year extends from May to November.

Table 9.2 shows the correlation coefficients of the monthly rainfall for major observation stations, obtained from the data taken for the period of May to November, generally considered as the rainy season. As can be seen, the data taken at the Ambuklao and Baguio City stations are very similar to those taken at the Binga station. It is there-

fore considered reasonable to make an estimate of the rainfall for the Binga damsite during the non-observation period on the basis of the data obtained for the same period at either the Ambuklao or Baguio City stations. The correlation coefficients of the monthly rainfall between the Binga and Baguio City stations and between the Binga and Ambuklao stations are plotted on Figs. 9.5 and 9.6, respectively.

The straight line shown in the Figures represents the linear regression line obtained from the data taken at the respective observation station. It can be expressed as:

$$R_{\text{BINGA}} = 157.2 + 0.899 R_{\text{AMBUKLAO}}$$

$$R_{\text{BINGA}} = 115.4 + 0.476 R_{\text{BAGUIO}}$$

Where,

R_{BINGA} is the monthly rainfall at the Binga damsite.

R_{AMBUKLAO} is the monthly rainfall at the Ambuklao damsite.

R_{BAGUIO} is the monthly rainfall at the Baguio City station.

Table 9.3 shows the monthly rainfall at the Binga damsite during the period from 1902 to 1986, by applying the above principles to estimate the rainfall during the non-observation period.

(2) Relation between Monthly Rainfall and Maximum Daily Rainfall at the Binga Damsite

Plotted on Fig. 9.7 is the relation between the monthly rainfall and maximum daily rainfall at the Binga damsite during the rainy season (May to November) for the period

during which the observation data were available (1970 to 1987). The straight line shown in the Figure represents the linear regression line of the monthly and maximum daily rainfall.

Table 9.3 shows the maximum daily rainfall at the Binga damsite obtained from the monthly rainfall over the period from 1902 to 1986.

(3) Relation between Daily Rainfall and Maximum Hourly Rainfall at the Binga Damsite

The hourly rainfall data at the Binga damsite are available only for the periods listed in Table 9.4. Plotted on Fig. 9.8 are the hourly rainfall data thus available for the period from July to October, 1980.

Table 9.5 shows the maximum rainfall (R_T) of consecutive hours ($T = 1$ to 12 hours) of the day with a maximum yearly rainfall. The table also shows the day's rainfall for 24 hours (R_{24}) and the rate of $T/24$.

The relation between the consecutive T -hour rainfall and the day's total rainfall is expressed as:

$$R_T = R_{24} \left(\frac{T}{24} \right)^K$$

The value K in this equation varies with the meteorological conditions of the region, but it may be shown by the straight line given in Fig. 9.9, in which the values for R_T/R_{24} and $T/24$ of Table 9.5 were plotted on a logarithmic paper. The value K is, therefore, estimated to be 0.76.

9.1.4. Water Levels, Inflows to and Outflows from the Binga Reservoir

(1) Record of Water Levels

Daily records on the water level of the Binga reservoir are available for the period from 1964 to 1987 (to September), while the hourly records are available for the principal flood season during the period from 1965 to 1986.

(2) Record of Reservoir Inflows

Daily records on the inflow to the Binga reservoir are available for the period from 1976 to 1987 (to March). The monthly records are available for the period from January 1962 to February 1987, while the annual records are available for the period from 1962 to 1986.

(3) Record of Reservoir Outflows

(i) Binga Reservoir

Daily records on the outflows from the Binga reservoir are available for the period from January 1964 to September 1987. Records on the spillway gate operation and water discharge through the spillway during floods are available for the period from 1964 to 1986.

(ii) Ambuklao Reservoir

Hourly records on the outflow from the Ambuklao reservoir during floods are available for the period from 1958 to 1986.

The period for which the above records are available is shown in Table 9.6.

(4) Hourly Inflows to the Binga Reservoir during Floods

The hourly inflows to the Binga reservoir during floods are obtained by considering the change of the reservoir water level and the amount of water released from the Ambuklao and Binga reservoirs during a given time. The floods considered in the calculation are limited to those which occurred in the period listed below, taking into account the magnitude of the floods and the period during which the respective data were available.

Period in which the Typical Magnitude Floods Occurred

<u>No.</u>	<u>Period</u>	<u>Maximum Inflow</u>	
1.	May 22 to 30, 1976	1,181.0 m ³	(May 26)
2.	June 25 to July 3, 1976	2,497.0	(June 30)
3.	November 1 to 7, 1980	2,617.0	(Nov. 5)
4.	August 28 to 31, 1984	2,498.8	(Aug. 27)
5.	June 22 to 25, 1985	902.5	(June 22)
6.	June 28 to July 1, 1985	1,258.8	(June 29)
7.	July 9 to 11, 1986	939.1	(July 11)

The inflows to the Binga reservoir were obtained using the following continuity equation:

$$dV/dt = Q_{inl} - Q_{out}$$

Or,

$$Q_{inl} = dV/dt + Q_{S1} + Q_{E1} \dots\dots (9.1.1)$$

When,

$$Q_{inl} = Q_{in2} + Q_{S2} + Q_{E2} \text{ and}$$
$$Q_{out} = Q_{S1} + Q_{E1}$$

Then,

$$Q_{in2} = dV/dt + Q_{S1} + Q_{E1} - (Q_{S2} + Q_{E2}) \dots (9.1.2)$$

Where,

- t = Time.
- V = Binga reservoir storage capacity.
- Q_{in1} = Inflow to the Binga reservoir.
- Q_{out} = Outflow from the Binga reservoir.
- Q_{S1} = Discharge through the Binga spillway.
- Q_{E1} = Releases through the Binga powerplant.
- Q_{S2} = Discharge through the Ambuklao spillway.
- Q_{E2} = Releases through the Ambuklao powerplant.
- Q_{in2} = Runoff inflow from the Binga dam basin
(drainage area), excluding Ambuklao dam basin.

Table 9.8 shows the hourly inflow to the Binga reservoir during typical flood periods obtained by using the above equation. Selected as typical floods are Nos. 1, 2 and 7 of Table 9.7. These floods were selected on the basis of their size and available data.

Fig. 9.10 shows the hourly inflow during the same typical flood periods. The inflows listed in Table 9.8 with negative sign are shown as zero in the above Figure.

9.1.5. Relation between Rainfall and Inflow

(1) Preparation of a Runoff Model

The runoff function method used for the Study of the Ambuklao Dam Rehabilitation Project is applied to the model to show the relation between the rainfall and water runoff.

The model was defined as follows:

$$Q = \left(\frac{r}{3.6}\right) Afa^2t \cdot \text{EXP}(-at) \dots \dots \dots (9.1.3)$$

where,

Q = Amount of runoff when rainfall r (mm/hr)
lasts one hour.

A = Drainage area (km²).
(246 km² in the case of the Binga dam basin.)

F = Runoff coefficient.

$\alpha = 1/tp$.

tp = Time lag (hr) from the beginning of rainfall until
the occurrence of peak runoff.

t = Elapsed time (hr).

A time-runoff curve (hydrograph) was obtained by applying
equation (9.1.3) using a series of different runoff
duration times.

The value "tp" in equation 9.1.3 was obtained by the
following method:

First, the flood wave velocity must be determined. The
flood wave velocity can be expressed, according to the
Rziha equation, as:

$$W = \left(\frac{h}{L}\right)^{0.6} \dots\dots\dots (9.1.4)$$

Where,

W = Flood wave velocity.

h = Difference in elevation between the upstream end
of the basin and the reservoir (m).

L = Distance from the upstream end of the basin to the
reservoir.

The concentration time of the flood, ta (sec.), can be
written as:

$$t_a = \frac{L}{W}$$

Where, for the Binga dam basin:

L is 34.32 km.

h is 1,715.0 m (EL.2.290 m - EL.575 m).

Hence,

$$W = 20 \times (1,715.0/34,320)^{0.6} = 3.31 \text{ m/sec.}$$

Therefore,

$$t_p = L/W = 34,320/3.31 = 10,368.58 \text{ sec.} = 2.9 \text{ hr.}$$

Conversion of the daily rainfall to the hourly rainfall can be accomplished by the following equation:

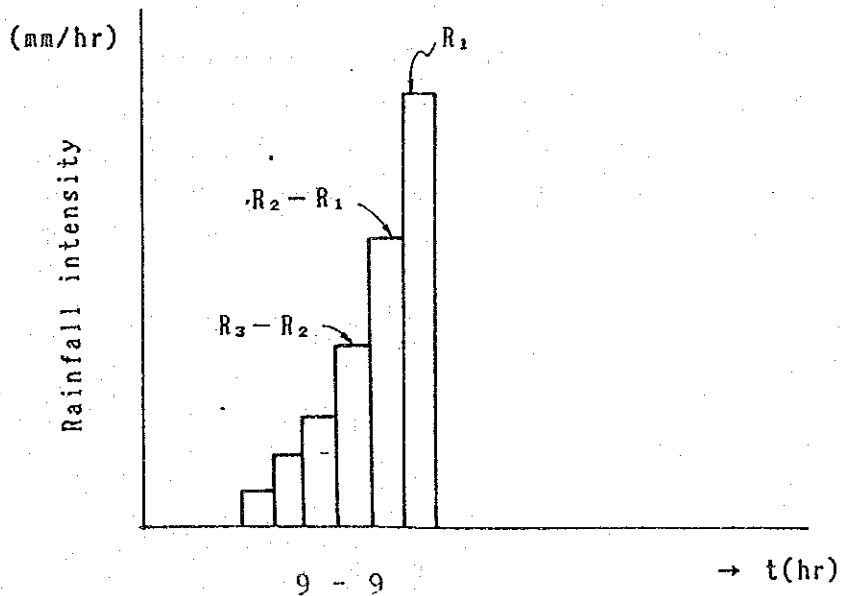
$$R_r \text{ (mm)} = R_{24} (t/24)^{0.76} \dots\dots\dots (9.1.5)$$

Where,

R_r = Rainfall for t hours.

R_{24} = Daily rainfall.

The rainfall for t hours (1,2,3, 24) can be obtained from the above equation, and the hourly rainfall can be determined by $R_1, R_2-R_1, R_3-R_2, R_4-R_3$ Shown below is a hyetograph composed on the basis of the results determined in the above manner.



The inflow to the Binga reservoir comprises the outflow from the Ambuklao reservoir and the runoff inflow of the Binga dam drainage area, excluding Ambuklao dam basin, and it can be written as:

$$Q_{in1} = Q_{in2} + (Q_{S2} + Q_{E2}) \dots\dots\dots (9.1.6)$$

where,

- Q_{in1} = Inflow to the Binga reservoir.
- Q_{in2} = Runoff inflow from the Binga dam drainage area.
- Q_{E2} = Releases through the Ambuklao powerplant.
- Q_{S2} = Discharge through the Ambuklao spillway.

(2) Verification

Plotted on Figs. 9.11 (1) to (3) are the inflow to the Binga reservoir during the three different flood periods, May 22 to 30, 1976, June 25 to July 3, 1976, and July 9 to 11, 1986. The calculated values are shown in these Figures by dotted lines and the measured values by solid lines.

In the calculations, the daily rainfall during the flood period was first converted to the hourly rainfall by using equation (9.1.5). For the 1986 flood period, the available measured hourly rainfall was used.

Next, runoff was calculated using equation (9.1.3). And finally, the inflow to the Binga reservoir was calculated using equation (9.1.6). In the calculations, the runoff coefficient was set at 0.8, and the base flow was assumed to be the average of the 25-year (1962 - 1987) flows of the respective months of the above flood periods.

9.1.6. Probable Flood Discharges for Various Return Periods

(1) Probable Daily Rainfall

The probable daily rainfall at the Binga damsite can be obtained from the data of the maximum daily rainfall during a year over the period from 1902 to 1984. The data contains the non-observation period from 1939 to 1946.

The Log-Normal, Moment and Gumbel-Chow Methods were used for the calculation. The results of the calculation are shown in Table 9.9 and are plotted on Fig.9.12 by Hazen Plot.

(2) Probable Inflow to the Binga Reservoir

The probable inflow to the Binga reservoir consists of the probable discharge from the Ambuklao reservoir and the runoff of the probable precipitation on the Binga dam basin excluding Ambuklao basin.

(i) Probable Discharge from the Ambuklao Reservoir

The probable discharge from the Ambuklao reservoir was estimated based on the maximum discharge through the spillway which may be produced by the following procedure of gate operation, as identified from several alternatives considered in the Study of the Ambuklao Dam Rehabilitation Project (JICA Report March 1988):

<u>Reservoir Water Level</u>	<u>Number of gates fully opened</u>
752.30	One
752.32	Two
752.34	Three
752.45	Four
752.50	Five
752.55	Six
752.60	Seven
752.65	Eight

The maximum inflow to and outflow from the Ambuklao reservoir by return periods are as shown below:

<u>Return Period</u>	<u>Maximum Inflow to the Reservoir</u>	<u>Maximum Discharge through the Spillway</u>
yrs	m ³ /sec.	m ³ /sec.
200	8,201	8,068
10,000	12,419	11,048

The probable discharge through the spillway for return period of 200 and 10,000 years in relation to time is as tabulated in the QS column of Table 9.10.

(ii) Maximum Probable Runoff Inflow from the Binga Dam Basin Excluding Ambuklao Dam Basin

The probable daily rainfall at the Binga damsite obtained in (1) above, and the rainfall pattern of five consecutive days for the period of May 23 to 27, 1976, Fig.9.13, in which the measured daily rainfall reached the maximum level throughout the year, were used for establishing the rainfall pattern of the corresponding return periods. The ratio of the maximum to the remainder in the pattern was identical to the actual pattern, Fig.9.13.

The maximum daily rainfall throughout the observation periods of 1971 to 1976, and 1980 to 1986 was 367 mm. It was recorded on May 25, 1976. The conversion of the daily rainfall to the hourly rainfall was made in a similar manner to that given in Para. 9.1.5(2), above.

The base flow was set at $15 \text{ m}^3/\text{sec}$. It was based on the monthly average for May of the years 1962 to 1987.

Also taken into account in the calculation was the discharge of $61.4 \text{ m}^3/\text{sec}$. corresponding to the Ambuklao plant power generation.

The maximum inflow to the Binga reservoir by return period was found to be:

$9,230 \text{ m}^3/\text{sec}$., for return period of 200 years
 $12,940 \text{ m}^3/\text{sec}$., for return period of 10,000 years

The results of the calculation as a function of time are shown in Table 9.10, and are plotted on Figs. 9.14 (1) and 9.14(2). These are flood inflow hydrographs for the Binga reservoir which depict the rate of inflow in relation to time (inflow-time curve).

9.2. Adequacy of Spillway Capacity

9.2.1. Spillway Capacity

The plan and the cross section of the spillway crest are shown in Fig.9.15. The relation between the reservoir water level and the discharge through the spillway for such shape, with the spillway gates fully open, is expressed, according to the Iwasaki Formula for standard overflow type crest sections, as follows:

$$Q = nCBH^{3/2} \dots\dots\dots (9.2.1)$$

$$C = 1.60 \frac{1 + 2a\left(\frac{H}{H_d}\right)}{1 + a\left(\frac{H}{H_d}\right)} \dots\dots\dots (9.2.2)$$

$$a = \frac{C_d - 1.6}{3.2 - C_d} \dots\dots\dots (9.2.3)$$

$$C_d = 2.2 - 0.0416\left(\frac{H_d}{W}\right)^{0.990} \dots\dots\dots (9.2.4)$$

Where,

Q = Discharge (m³/sec.)

n = Number of spillway gates.

B = Width of the overflow section (m).

H = Head measured from top of the crest (m).

H_d = Design head measured from top of the crest (m).

W = Height of the weir.

a = Constant.

C = Discharge coefficient.

C_d = Discharge coefficient when H = H_d

The characteristics of the Binga spillway gates are:

Crest level : EL.563.0 m (2)

Number of gates : 6 (n)

Width of gate : 12.5 m (B)

Height of weir : 6.0 m (W)

Width of pier : 4.121 m (b)

The discharge coefficient for the design normal water level in the reservoir at EL.575.0 meters was obtained by the use of the Iwasaki Formula as follows:

$$H_d = \text{NWL EL.575.0 m} - \text{EL.563.0 m} = 12 \text{ m}$$

$$W = 6 \text{ m}$$

$$\text{Therefore, } C_d = 2.200 - 0.0416\left(\frac{12}{6}\right)^{0.990} = 2.1174$$

Using equation (9.2.3), the corresponding value for "a" is obtained as follows:

$$a = \frac{2.1174 - 1.6}{3.2 - 2.1174} = 0.4779$$

The value of "C" is obtained by equation (9.2.2) assuming $H = H_d$:

$$C = 1.60 \times \frac{1 + 2 \times 0.4779}{1 + 0.4779} \div 2.1174$$

By applying equation (9.2.1) using the above values, the discharge over the spillway crest for the reservoir water level at EL.575.0 meters is:

$$Q = 6 \times 2.1174 \times 12.5 \times 12^{3/2} = 6.600 \text{ m}^3/\text{sec.}$$

The relation between the partial opening of the spillway gates and the water discharge can be expressed as:

$$Q = \frac{2}{3} \sqrt{2g} \mu B (H_1^{3/2} - H_2^{3/2})$$

Where,

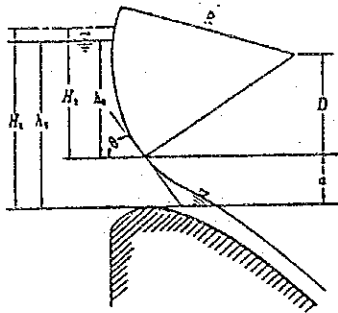
μ = Discharge coefficient (see Fig. shown below).

B = Width of gate.

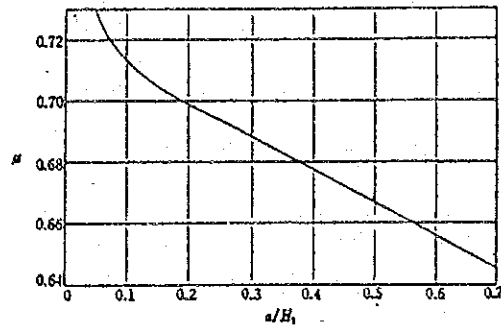
H_1 = Total head on the crest, including velocity head.

H_2 = Total head on the gate bottom.

For illustration, see sketch below.



Cross section of spillway crest with partial gate opening



Discharge coefficient for partial gate opening (USBR)

The relationship between the discharge and the gate opening for various reservoir water levels is shown in Fig.9.16.

9.2.2. Maximum Rise of the Reservoir Water Level

The maximum rise of the reservoir water level has a direct bearing on the adequacy of the required safe freeboard for the dam. The required freeboard is greatly influenced by the effects of floods, winds and earthquakes.

(1) Rise of the Level due to Floods (Maximum Flood Surge)

Flood studies were conducted for floods with a 200-year and 10,000-year return periods. The corresponding maximum inflows (peak of the inflow hydrograph) were 11,080 m³/sec (increased by 20% over the 200-year flood inflow), and

12,940 m³/sec, respectively. The results of the studies are shown in Figs. 9.17 (1) through 9.17(4).

The studies were based on the assumption that the gates will be operated in the following manner:

Gate operation procedure "A"

The first two gates are fully open when the water level reaches EL.575.3 m

The next two gates are fully open when the water level reaches EL.575.5 m

The last two gates are fully open when the water level reaches EL.575.7 m

Gate operation procedure "B"

This procedure consists of gate operation procedures currently used at the Binga dam based on the existing Flood Operation Rule for the Binga Dam. The relationship between the reservoir water level and the spillway discharge is shown in Fig.9.18.

The maximum water levels at the time of the maximum probable inflow are given below. There are practically no differences between the corresponding reservoir levels for the above two cases, i.e., gate operation procedure "A" and "B".

Flood Frequency	Max. Inflow (m ³ /s)	Gate Operation Procedure "A"		Gate Operation Procedure "B"	
		Max. Discharge (m ³ /s)	Max. Reservoir Level (EL m)	Max. Discharge (m ³ /s)	Max. Reservoir Level (EL m)
1/200 x 1.2	11,080	11,050	579.329	11.050	579.339
1/10,000	12,940	12,840	580.878	12.840	580.878

(2) Waves due to Winds and Earthquakes

(i) Waves due to Winds

The Sverdrup-Munk-Bretschneider (SMB) equation was used to determine the height of the wave generated by wind.

$$h_w = 0.00086 v^{1.1} F^{0.45}$$

Where,

h_w = Height of wave due to wind.

v = Wind velocity (m/sec), average of 10 minutes.

F = Fetch (km).

For the calculations, wind velocity at the Binga damsite was set at 50 m/sec, which corresponds to the maximum recorded at the Baguio observation station, although the maximum velocity recorded at the site was only 36 m/sec (July 19, 1986). The fetch was set at 1,400 m based on the plan shown in Fig.10.1.

When the above values are applied to the SMB equation, the following is obtained:

$$\begin{aligned} h_w &= 0.00086 \times 50^{1.1} \times 1,400^{0.45} \\ &= 1.656 \text{ m} \doteq 1.70 \text{ m} \end{aligned}$$

(ii) Waves due to Earthquakes

The equation by Dr. Sato was used for determination of the height of the wave generated by earthquake.

$$h_e = \frac{1}{2} \times \frac{K}{\pi} \sqrt{gH_0}$$

where,

he = Height of wave above reservoir water surface
due to earthquake.

k = Seismic coefficient of the dam at normal water
level, 0.15.

π = Seismic period, 1 sec.

Ho = Depth of reservoir water at normal level.

Since the bottom of the Binga reservoir is currently
at EL.530 meters, Ho is computed to be 45 meters
(EL.575 - EL.530).

Thus,

$$h_e = \frac{1}{2} \times \frac{0.15 \times 1}{3.14} \sqrt{9.8 \times 45} = 0.502 \text{ m} \approx 0.50 \text{ m}$$

The combined height of the waves due to wind and
earthquake were, therefore, found to be:

$$1.70 + 0.50 = 2.20 \text{ m}$$

The above waves plus the maximum reservoir water level
for floods with frequency of 1/200 multiplied by 1.2
and for floods with frequency of 1/10,000, will
produce levels at EL.581.539 and 583.078 meters,
respectively.

Since the dam crest is at EL.586 m, the dam will still
have a freeboard of 4.461 and 2.922 meters above the
two above reservoir levels, respectively.

9.2.3. Conclusions

As described in Para. 9.2.2(1), the maximum discharge from the

Binga reservoir and the maximum reservoir water level for a 1/200-frequency flood multiplied by 1.2, which actually corresponds to the 1/1,000 frequency flood, are 11,050 m³/sec, and EL.579.34 m, respectively. The corresponding values for the 1/10,000-year frequency flood are 12,840 m³/sec, and EL.580.88 m.

As also described in Para 9.2.2(2), the freeboard for the Binga dam was established to be 4.46 and 2.92 meters for floods with 1/1,000 and 1/10,000 return periods, respectively. The freeboard was computed assuming simultaneous occurrence of waves due to wind and earthquake.

The above freeboards developed for two major flood frequencies are considered to be acceptable. Therefore, the dam and the spillway are regarded to be safe and adequate for the above two floods.

9.3. Plunge Pool

9.3.1. Spillway Discharges

Table 9.11 gives the average daily spillway discharges greater than 1,000 m³/sec and the maximum spillway discharge for the respective days. These are recorded spillway discharges for the period from August 1964 to October 1986.

In accordance with the records, the serious damage to the retaining wall installed for protection of the downstream end (toe) of the dam occurred on July 1, 1976.

The peak inflow of the flood occurred a day before, June 30, 1976. The maximum discharge through the spillway during this event was 2,602 m³/sec, which also was the maximum to ever pass over the Binga spillway.

9.3.2. Plunge Pool Depth

Shown in Fig.9.19 is a longitudinal profile of the plunge pool along the extension of the spillway chute centerline on the basis of the topographic survey made in 1987. The dotted line in the above Figure depicts the estimated trajectory of the jet produced by the action of the flip bucket located at the downstream end of the spillway chute. The trajectory corresponds to a flip bucket angle of 30° and a velocity of 31 m/sec. Fig.9.20 shows the estimated water levels at the downstream end of the pool for the spillway discharge of 6,600 m^3/sec , occurring when six gates are fully open at NWL, and 2,602 m^3/sec , corresponding to the flood which damaged the retaining wall. The water levels were determined by non-uniform flow calculations with the Manning's roughness coefficient (n) of the riverbed assumed equal to 0.04.

On the basis of the above calculations, it is assumed that the jets corresponding to discharges of 6,600 m^3/sec and 2,602 m^3/sec would land in the pool at points 108 and 114 m downstream of the tip of the flip bucket. The water depths in the pool during above discharges would be 25 to 30 m.

9.3.3. Flow Regime in the Plunge Pool

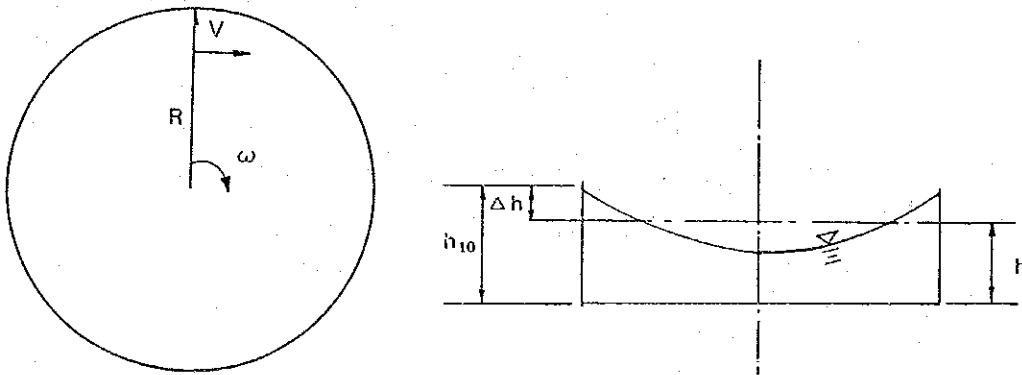
(1) Flow Velocities

(i) Hydraulic Model Studies

The spillway discharges would cause a fluctuating and complicated flow regime in the plunge pool when the jet trajectory produced by the flip bucket would hit the pool area consisting of irregular and uneven topography.

Therefore, hydraulic model studies were conducted to determine the most suitable rehabilitation measures to be provided for the damaged protection wall of the dam. The model could reproduce similar flow regime to the above. The model was based on conservative assumptions compared with the actual design of the structures.

The topography of the plunge pool is shown in Fig.9.21 (plan), and Fig.9.22 (cross sections). It was possible to make a good approximation of the actual topography on the adopted model tank of a round shape shown below.



(ii) Velocity at the Flip Bucket

The velocity of the flow at the spillway flip bucket was obtained from the graph shown in Fig.9.23.

The meaning of the symbols in Fig.9.23 is as follows:

V_1 = Flow velocity at the invert of the flip bucket.

Z = Total head ($H_o - H_d$).

H_o = Reservoir water level.

H = Head on the spillway crest (reservoir level minus crest level).

H_d = Water surface level at the invert of the flip bucket ($Y_1 + Z_1$).

y_1 = Depth of flow at the invert of the flip bucket.

Z_1 = Elevation of the invert of the flip bucket.

The values of the above symbols for the Binga spillway are:

$$H_o = 575.0 \text{ m}$$

$$Z_1 = \text{EL.}512.739 \text{ m}$$

$$H_d = \text{EL.}516.549 \text{ m}$$

$$y_1 = 3.81 \text{ m}$$

$$H \doteq 12 \text{ m}$$

$$Q = 6,600 \text{ m}^3/\text{sec.}$$

Using the above values in the graph shown in Fig. 9.23, the velocity at the flip bucket invert for a spillway discharge of $6,600 \text{ m}^3/\text{sec}$ is found to be 31 m/sec .

(iii) Velocity of the Jet at the Impact Area of the Plung Pool

Velocity of the jet in the impact area of the plunge pool was determined by the following equations:

$$q = Q/B$$

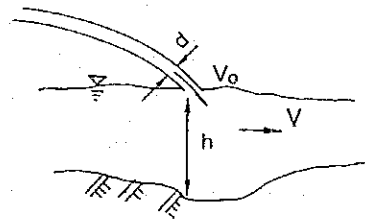
$$d = g/V_o$$

$$h = \frac{d}{2}(\sqrt{1 + 8Fr_1^2} - 1)$$

$$Fr_1 = \frac{V_o}{\sqrt{gd}}$$

Then,

$$V = \frac{q}{H}$$



Where,

Q = Discharge.

B = Width of the flip bucket.

d = Thickness of the jet.

q = Flow per unit width of the bucket.

h = Conjugate depth in the jet impact area of the plunge pool immediately before impact, assumed to be the maximum depth of the pool.

V_0 = Velocity of the jet immediately before impact.

V = Velocity of the jet immediately after impact.

The corresponding quantities for the above symbols for the Binga plunge pool are:

$$Q = 6,600 \text{ m}^3/\text{sec}$$

$$B = 55.828 \text{ m}$$

$$V_0 = 31 \text{ m/sec}$$

Therefore,

$$q = 6,600/55.828 = 118.220 \text{ (m}^3/\text{sec)}$$

$$d = 118.220/31 = 3.814 \text{ (m)}$$

Using the above formula and quantities, the following is obtained:

$$Fr_1 = \frac{31}{\sqrt{9.8 \times 3.814}} = 5.07$$

Thus,

$$h = \frac{3.814}{2} \times (\sqrt{1 + 8 \times 5.07^2} - 1) = 25.50 \text{ (m)}$$

and

$$v = \frac{118.220}{25.5} = 4.64 \text{ m/sec}$$

The maximum velocity at the impact area of the plunge pool should, therefore, be considered to be about 5 m/sec.

(iv) Operating Water Levels in the Plunge Pool

The maximum depth in the model tank for the plunge pool is expressed as:

$$h_m = h + \frac{\omega^2 R^2}{4g}$$

When,

$$\Delta h = h_m - h,$$

Then,

$$\Delta h = \frac{\omega^2 R^2}{4g}$$

Where,

h = Average water depth in the model tank.

h_m = Maximum water depth in the tank.

ω = Angular velocity of the circulating flow in the tank.

R = Radius of tank.

g = Acceleration of gravity.

Assuming R to approximately be equal to 70 m and V equal to 5 m/sec for the model tank,

then,

$$\omega = \frac{V}{R} = \frac{5}{70} = 0.07 \text{ radians/sec}$$

and,

$$h = \frac{0.07^2 \times 70^2}{4 \times 9.8} = 0.613 \text{ (m)}$$

For the design of the required protection measures for the downstream end of the dam (toe of the dam), it is important to determine the maximum probable water levels at this location. The maximum water level should include the above increase in the water level, plus the velocity head, which in this case is $V^2/2g$ or $5^2/19.6$ (1.28 m).

As a result of the above studies, the water levels at the toe of the dam are as shown below:

<u>Spillway Discharge</u> (m ³ /sec)	<u>Water Level</u> (meters)
6,600	EL.497.5 + 0.613 + 1.28 = 499.393 m or, \doteq 500.0 m
2,602	EL.492.5 + 0.613 + 1.28 = 494.393 m or, \doteq 495 m

(2) Size of Rock for the Proposed Rockfill Protection of Dam Toe

The size of the rock for the rockfill to be used for protection of the dam toe at the location of the demolished retaining wall, required to resist a velocity of 5 m/sec, shall be determined as follows:

$$V = \frac{1}{n} h^{2/3} i^{1/2}$$

Where,

n = Assumed 0.05.

h = Average water depth at the retaining wall. Based on the water level at the retaining wall as determined by the model (EL.500 m) and the riverbed elevation at that location (EL.492 m), "h" is assumed equal to 8 meters.

Then,

$$i = \left(\frac{V \times n}{h^{2/3}} \right)^2 = \left(\frac{5 \times 0.05}{8^{2/3}} \right)^2 = 3.852 \times 10^{-3}$$

In order to use Iwagaki's formula, the value of U^* must be determined as follows:

$$U^* = \sqrt{ghi} \quad \text{or,}$$

$$U^* = \sqrt{9.8 \times 8 \times 3.852 \times 10^{-3}} = 0.550 \text{ m/sec.}$$

By using the Iwagaki formula $U^*C^2 = 80.9d$, the size of the rock for the rockfill protection is determined:

$$d = \frac{U^*C^2}{80.9} = \frac{(0.550 \times 100)^2}{80.9} = 0.374 \div 0.5 \text{ m}$$

The rock size for the protection rockfill can also be obtained from the Ishash formula. The formula was established on the experimental basis to determine the size of a rock of a rockfill dike in a stream which could withstand various stream flow velocities.

The minimum velocity required to move loose rock in a stream can be expressed, according to the W. Airy's formula, as:

$$V_{\min} = E_1 N \sqrt{D}$$

Where,

V_{\min} = Minimum velocity required by the stream to move a rock of a specific size.

$$N = 2g \frac{\Delta 1 - \Delta}{\Delta}$$

E_1 = Non-dimensional coefficient (0.86, according to the Ishash experiment).

$\Delta 1$ = Specific gravity of the rock.

Δ = Specific gravity of the water.

D = Diameter of the rock
(on the assumption that it has a spherical shape).

When,

$$V_{\min} = 5 \text{ m/sec, } \Delta 1 = 2.65 \text{ and } \Delta = 1.0,$$

Then,

$$N = 19.6 \times \frac{2.65 - 1.0}{1.0} = 5.687$$

Hence,

$$D = \left(\frac{V_{\min}}{E_1 N} \right)^2 = \left(\frac{5}{0.86 \times 5.687} \right)^2 = 1.045 \text{ (m)}$$

Based on the above, it is determined that the size of the rock for the rockfill protection of the dam toe should be between 0.5 to 1 meter.

9.3.4. Conclusions

The water level in the plunge pool at the location of the damaged retaining wall would be at EL.500.0 m at the time of spillway discharge of 6,600 m³/sec. with the spillway gates fully open, and the normal reservoir water level (NWL) at EL.575 m. The rock to be used for construction of a protective

rockfill at the toe of the dam where the present, demolished retaining wall is located, should have a size of 0.5 to 1.0 meter. The above is considered to provide adequate protection for the downstream end of the dam.

10. RESERVOIR SEDIMENTATION

10. Reservoir Sedimentation

The principal purpose of the studies presented in this Section is to confirm the progress over the past years of sediment inflow and deposition in the Binga reservoir and to forecast the future trends of sedimentation.

Deposition of sediments in the upstream portions of the Binga reservoir has resulted in increase of the level of the riverbed in the area around the outlet of the Ambuklao tailrace, thus causing problems for proper and unrestricted power generation of the Ambuklao power plant. Study of the measures to remove the sediments from this area by special discharging operations of the Ambuklao spillway is also included in this Section.

10.1. Sedimentation Data

10.1.1. Cross Sections of the Reservoir

In the past, a depth survey of the Binga reservoir was made three times in 1967, 1979 and 1986. Shown in Figs. 10.2(1) through 10.2(8) are the cross sections of the reservoir based on the 1986 survey along the measurement lines given in Fig.10.1. Shown in Fig.10.3 are the longitudinal profiles of the reservoir bed based on the 1967, 1979 and 1986 surveys.

10.1.2. Sediment Properties

(1) Grain Size Distribution

Samples were taken at nine locations, as shown in Fig.10.4, to investigate the grain size distribution, specific gravity and unit weight of the reservoir sediment materials.

Shown in Figs.10.5(1) through 10.5(3) are the grain size distribution curves prepared on the basis of the results of the investigation. Two types of samples were collected for this investigation. One type consisted of sediments with gravel size greater than 100 mm, while the other type comprised sands and gravels smaller than 100 mm. The curves were based on the results of the studies of these samples.

(2) Specific Gravity and Unit Weight

The specific gravity of the sample materials collected from the sampling points were in the range of 2.66 to 2.83. The unit weight was in the range of 1.92 to 2.18 g/m³. Table 10.1 shows the specific gravity and unit weight of the materials by sampling location.

10.1.3. Changes in the Reservoir Storage Capacity

Shown in Fig.10.6 are the Binga reservoir storage capacity curves for the years 1960, 1967, 1979 and 1986, prepared on the basis of the data given in the Binga Hydro Reservoir Sedimentation, an information on Binga reservoir sedimentation compiled by NPC.

Given below are the changes by year in the gross, effective and dead storage capacities of the reservoir and in sedimentation:

<u>Year</u>	<u>Gross Storage Capacity</u>	<u>Effective Storage Capacity</u>	<u>Dead Storage Capacity</u>	(10 ⁶ m ³)
				<u>Sedimentation</u>
1960	87.445	45.887	41.556	0
1967	81.889	44.070	37.819	5.554
1979	64.843	35.103	29.740	22.600
1986	56.119	36.173	19.946	31.324

The progress of sedimentation over the 26-year period from 1960 to 1986, given above, indicates that the annual average rate of sediments (average sediment yield) and the specific sediment rate (sediment yield rate) are $1,205 \times 10^6 \text{ m}^3$ and $4,897 \text{ m}^3/\text{Yr}/\text{km}^2$, respectively.

Shown in Fig.10.8 is the comparison of the Binga specific sediment rate with those of other river basins. As shown in the above Figure, the Binga specific sediment rate is comparatively smaller than that for the Ambuklao.

10.1.4. Sedimentation Trends

Shown in Fig.10.7 is the progress of sedimentation and the volume of sediments in the reservoir for the years 1967, 1979 and 1986.

The accumulated amount of sediments totals $11.8 \times 10^6 \text{ m}^3$ for the period from 1967 to 1979, and $14.3 \times 10^6 \text{ m}^3$ for the period from 1979 to 1986.

Sedimentation delta in the reservoir has been created by deposition of sands and gravels with a coarse grain size greater than 0.1 to 0.2 mm. These sands and gravels were produced in the Binga drainage area, transported to the reservoir, and deposited along the reservoir bed in accordance with the size of the suspended sediment and the velocities in the reservoir. The size of the deposited sediments decreased gradually toward the downstream end of the reservoir as affected by the depth of the reservoir and the corresponding velocities.

As shown in Fig.10.7, the sedimentation delta in the reservoir consists of the topset beds, upstream of the peak of the delta and the foreset beds, immediately downstream of the peak characterized by a steep gradient.

The sedimentation delta moves downstream toward the dam with passing of time. Downstream of the foreset beds of the sedimentation delta, there are wash loads with a grain size smaller than 0.1 mm. The deposits with a gentle gradient are called bottomset beds, and the deposits extending toward the dam, created by movement of wash loads by density currents, are called density current beds.

Based on the formation of the sedimentation as mentioned above and the change in the sedimentation profile by year, the accumulated amount of sediments can be divided into three sections as given in the following tabulation.

<u>Reservoir Section</u>	<u>Period</u> <u>1967 to 1979</u>		<u>Period</u> <u>1979 to 1986</u>	
	<u>Sand and</u> <u>Gravel</u>	<u>Silt</u>	<u>Sand and</u> <u>Gravel</u>	<u>Silt</u>
	Upstream from the Adonot River	1.257		0.038
Between the Adonot and Sadyo Rivers	7.961	1.475	3.541	5.672
Downstream of the Sadyo River		1.102		5.064
Total	11.8		14.3	

(10⁶ m³)

10.2. Forecast of Sedimentation Progress

10.2.1. Calculation Methods and Formulae

The calculation methods and formulae used for the forecast were:

- (1) One-dimensional analysis of movement of flows and sediments in the reservoir.

- (2) Non-uniform flow calculation method for the calculation of water flow rates.
- (3) The Shinohara-Tsubaki's formula for the calculation of sand flow rates of the bedload.
- (4) The Lane-Kalinske's formula for the calculation of sand flow rates of the suspended load.

The wash loads were taken into consideration in applying the continuity equation.

10.2.2. Verification of Calculations

A bathymetric survey of the reservoir was actually made in both years of 1979 and 1986 as mentioned previously. The actual progress of sedimentation over this seven-year period was analyzed by simulation to verify the model used for calculations.

The comparison of the calculated results with the actual values is shown in Fig.10.9. As is seen, a relatively satisfactory reproduction by simulation of the 1986 survey results, was possible.

The assumptions used in the above calculations were described below:

(i) Cross Sections of the Reservoir Bed during the Initial Period (1979)

A trapezoidal shape cross-sections of the reservoir bed was used for the model for the calculations. There are 36 cross-sections of the downstream portions which covered seven kilometers length of the reservoir. Their characteristics are shown in Table 10.2.

(ii) Water Flow Regime

The flow regime for the year 1981 was used as the average annual flow for the calculations, as the annual runoff for this year is considered to be a mean of the seven-year period from 1979 to 1986. The maximum daily flow rate for the year 1981, according to the Gumbel-Chow Method, is equivalent to a flood with a 2.5-year return period. This corresponds to the dominant discharge rate of a river that has a dominant effect on the formation of the river configuration which is equivalent to a flood with a return period of 1.07 to 4.0 years.

A peak flood discharge of $1,544.4 \text{ m}^3/\text{sec}$ was used. This was obtained from the relation between the average daily inflow, $933.8 \text{ m}^3/\text{sec}$ as recorded in 1981, and the maximum daily inflow, as shown in Table 10.3 and Fig.10.10.

The input data used in the calculations were only those exceeding $100 \text{ m}^3/\text{sec}$ (38 days in 1981). They were indicated in two peak patterns as shown in Fig.10.11.

The inflow data were divided into three rivers, Sadyo, Adonot and Agno, in proportion to the respective catchment areas as given in Table 10.4. The same flow regime was repeated for every year considered.

(iii) Reservoir Water Level

The initial water level each year considered in the calculations was assumed to be at EL.555 m, taking into consideration the Binga plant operating practice of lowering the reservoir level to the low water level (L.W.L.) prior to the rainy season.

The water level was determined on the basis of the relation between the inflow and the amount of water required for power generation ($88 \text{ m}^3/\text{sec}$).

In case when the water level exceeded the elevation of the spillway crest, EL.563 m, the resulting water levels were determined by considering the water discharges through the spillway.

(iv) Grain Size Distribution

The grain size distribution in the recent sedimentation deposits as given by Sample No.8 shown in Fig.10.5 was applied to a section of the reservoir between Cross Sections 11 and 35, and that of Sample No.9, to the reservoir section between Cross Sections 0 and 10. The distribution was recalculated after excluding silts (wash loads) composed of grains with a size smaller than 0.061 mm, as shown in Table 10.5 and Fig.10.12.

(v) Sediment Inflow

The annual average sediment inflow (sediment yield) of $2.0450 \times 10^6 \text{ m}^3$ over the period from 1979 to 1986 was applied as the input data for the calculation of the annual sediment inflow. By size of grain, this was divided as follows:

Silt : $1.5337 \times 10^6 \text{ m}^3/\text{Year}$
Sand and gravel : $0.5113 \times 10^6 \text{ m}^3/\text{Year}$

The silt inflow was divided in proportion to the respective catchment areas of Sadyo, Adonot and Besal rivers. On the other hand, only Adonot and Besal catchment areas comprised the sand and gravel inflows, since Sadyo river mouth does not have any evidence of a

substantial amount of deposition nor was there any such inflow from the Ambuklao reservoir.

As a result, the sediment inflow from each river basin by grain size is estimated to be as shown in the tabulation given below:

River or Reservoir	Catchment Area (km ²)	Silt (10m ⁶ m ³ /yr)	Sand and Gravel 10m ⁶ m ³ /yr)
Sadyo	2.5	0.0049	-
Adonot	69.0	0.1131	0.1449
Besal	174.5*	0.2851	0.3664
Ambuklao	690.0	1.1306	-
Total	936.0	1.5337	0.5113

Note: The number marked with an asterisk includes a combined catchment area of 27.5 km² of other than Sadyo, Adonot and Besal tributaries.

10.2.3. Future Sedimentation

(1) Anticipated Progress of the Reservoir Sedimentation

Shown in Fig.10.13 is the calculated expected sedimentation in the reservoir for the period from 1986 to 2022. The changes to the reservoir storage capacity as affected by the anticipated sedimentation increase during the above period are shown in Table 10.6. These changes are also graphically presented in Fig.10.14.

The rate of progress of sedimentation in the reservoir until the year 2010 is estimated to be about 200 m/year.

The rate of increase in the level of sediments in the power intake area (Cross Section No.1) until the year 2015 is estimated to be 0.8 m/year.

The tabulation given below presents the changes, by typical year, in the gross, effective and dead storage capacities of the reservoir and in the level of sediments.

Typical Year	Gross Storage Capacity (10^6 m^3)	Effective Storage Capacity (10^6 m^3)	Dead Storage Capacity (10^6 m^3)	Elevation of Sediments at the Intake Structure (El.m)
1986	60.83	38.93	21.90	528.453
1990	55.00	37.03	17.97	531.355
2000	41.56	31.94	9.62	539.267
2010	28.65	26.58	2.07	547.894
2015	22.45	22.18	0.27	552.067

The above calculations were based on the following assumptions:

(i) Cross Sections of the Reservoir Bed during the Initial Period (1986)

A trapezoidal shape was used for the calculation model. The number of Cross Sections of the downstream portion of the reservoir used in the calculation was 36. Their characteristics are given in Table Nos. 10.7(1) and 10.7(2).

(ii) Reservoir Water Level

For the purposes of analysis, the initial reservoir water level for 1986 was assumed to be at the minimum reservoir operating water level (L.W.L.), EL.555 m.

The initial water level for the 1987 and the years thereafter was also assumed to be L.W.L. as long as the reservoir bed level around the power intake (Cross Section 1) remained below the intake level (EL.540 m). For cases when the reservoir bed around the power intake reaches and exceeds the intake level, the initial water level was assumed to be 15 m (the difference between the reservoir L.W.L. and the intake level, or EL.555 m - EL.540 m) above the reservoir bed level at the intake, assumed to exist in the year under consideration.

(iii) Sediment Inflow

The annual average sediment inflow (yield) of $1.3742 \times 10^6 \text{ m}^3$ over the period from 1967 to 1986 was used as the input data for the calculation of the annual sediment inflow. By size of grain, this was divided as follows:

Silt	:	$0.7007 \times 10^6 \text{ m}^3/\text{year}$
Sand and gravel	:	$0.6735 \times 10^6 \text{ m}^3/\text{year}$

Division of the sediment inflow between the Sadyo, Adonot, Besal and Agno Rivers, by grain size, was made in accordance with the procedure described in Section 10.2.2.(v).

- (iv) These calculations were based on the evaluation of the water flow regime and grain size distribution as described in Section 10.2.2, above.

(2) Anticipated Progress of the Sedimentation in the Upstream Portions of the Reservoir

Shown in Fig. 10.15 is the anticipated progress of the

reservoir sedimentation at the tailrace outlet of the Ambuklao powerplant located at the upstream end of the reservoir.

The change in the level of the reservoir bed at the Ambuklao tailrace outlet was determined on the basis of the change in the level of the reservoir bed at the location where the Adonot River enters the reservoir (Cross Section 34). This can be done on the assumption that the gradient of the reservoir bed in the section between this location and the Ambuklao tailrace outlet remains unchanged from the conditions assumed in the analysis (the year 1987 conditions). This means that the gradient of the reservoir bed in this section has achieved by now its state of equilibrium and that this equilibrium will also be maintained in the future.

The possible effect on the water levels in the Ambuklao surge tank by further accumulation of sedimentation on the reservoir bed in the area around the Ambuklao tailrace outlet is shown in Fig.10.16. It shows the relation between the time required for sudden load increase from startup to full load (For flows from 0 to $61.4 \text{ m}^3/\text{sec}$) and the increase or decrease in the water levels of the surge tank due to surges (the difference between the maximum water level and the level of the valve chamber invert, or the difference between the minimum water level and the level of the orifice of the surge tank base).

As can be seen from the above Figure, it is possible to prevent the surging water inflow into the valve chamber by maintaining the time required for sudden load increases (0 to $61.4 \text{ m}^3/\text{sec}$) over 100 seconds. This can still be accomplished even when the reservoir bed immediately downstream of the Ambuklao tailrace outlet would reach the levels as anticipated for the year 2022.

On the other hand, it is possible to prevent air inflow into the tailrace tunnel by maintaining the time required for sudden load increase (0 to 61.4 m³/sec) over 180 seconds for the present level of sedimentation (1987).

The minimum opening time for the Ambuklao turbine inlet gates required to maintain the water level in the surge tank at levels lower than EL.604.0 m and higher than EL.579.6 m, during sudden load increases, are given in the tabulation below:

<u>Year</u>	<u>Minimum Gate Opening Time</u>	<u>Surging Restriction</u>
1987	190 sec.	Downward surging
2000	170	- do -
2010	90	- do -
2020	90	Upward surging

The change in the gate opening time is plotted on Fig.10.17.

The input variables for the calculation of the above relations were as follows:

- Water level at the tailrace outlet : EL.579.061 m
- Roughness coefficient for the tailrace tunnel: 0.013(n)
- Total length of the tailrace tunnel: 2,201.035m(ℓ)
- Tunnel cross section: Circular with a diameter of 5 m.

Note: The water level at the tailrace outlet was obtained by non-uniform flow calculation for the river section between the upstream end of the Binga reservoir and the Ambuklao tailrace outlet. These calculations were performed for a discharge of $Q = 61.4 \text{ m}^3/\text{sec}$, corresponding to three turbines operating simultaneously at full gate opening. The installed capacity of the Ambuklao power plant is 3

units, 25 MW each. Manning's roughness coefficient (n) at 0.030, and the Binga reservoir NWL at 575.0 m. Twenty seven cross sections along the reservoir bed were used for the above calculations.

On the basis of the above calculations, the following conclusions are made:

- (i) The year in which the sedimentation will reach the power intake at EL.540 m would be 2000.
- (ii) The year in which sands and gravels begin to enter the power intake would be 2015.
- (iii) The year in which the sedimentation could reach the level of the spillway crest would be 2022.
- (iv) The sedimentation at the Ambuklao tailrace outlet may not cause any surging problems, if the sudden load increase is handled in a prudent manner, i.e., gate opening time longer than 180 seconds for the present level of sedimentation, and gate opening time longer than 90 seconds for the sedimentation level anticipated to occur in 2020. The above turbine gate operating requirements will keep the operation of the surge tank within acceptable limits.

10.3. Sedimentation at the Upstream Reaches of the Binga Reservoir

In this section, countermeasures against the sediments accumulated at the upper reaches of the Binga reservoir, particularly around the Ambuklao tailrace outlet, were studied and compared as required. The sediments so accumulated raised the elevation of the riverbed level, thereby affecting the power generation of the Binga plant. The countermeasures consist of the following two alternative methods:

- Removal of the sediments by operating the Binga and the Ambuklao reservoirs.
- Dredging of the sediments along the relevant river course.

10.3.1. Removal of the Sediments by the Reservoir Operations

(1) Cross Sections of the Upstream Reaches of the Reservoir

Shown in Figs. 10.19(1) to 10.19(7) are the cross sections of the upstream portion of the Binga reservoir based on the 1987 survey along the measurement lines given in Fig.10.18.

(2) Method to Remove the Sediments by Reservoir Operation

Flushing out of the sediments from the area immediately downstream of the Ambuklao tailrace outlet was studied by simulating the effects of the water discharges through the Ambuklao spillway on the sediments at the upstream end of the reservoir (Cross Section T-31).

The results of the studies are shown in Figs.10.20 and 10.21. Fig.10.20 shows the change in the longitudinal profiles of the reservoir bed. As is seen, the reservoir bed upstream of the tailrace outlet is scoured off and the sediments are moved downstream. Fig.10.21 shows the change with time of the sediment depth in the area around the tailrace outlet by scouring (Cross Section T-27). As is seen, a discharge greater than $2,000 \text{ m}^3/\text{sec}$ would scour the reservoir sediment deposits to a greater depth. The maximum scoured depth would amount to about 1.23 m.

Shown in Fig.10.22 is the change in the scoured depth of the sediment deposits around the tailrace outlet by repeated (sequence of three times) spillway discharging

operation. It can be seen from this Figure that the scouring depth gets smaller with each subsequent operation of the spillway due to increased consolidation of the reservoir sediments (increased resistance to erosion).

The following data and assumptions were used in making these calculations:

(i) Cross Sections of the Reservoir Bed

Reservoir Cross Sections T-1 to T-31 for the upstream portion of the reservoir, made by the 1987 survey, and Cross Sections 0 to 30 for the downstream portion, made by the 1986 survey and as shown in Fig.10.2, were used for the calculation model. Table 10.8 shows the main characteristics of each cross section.

(ii) Water Inflow

The water inflow at the upstream end of the reservoir was calculated on the basis of a curve showing the outflow rate (discharge per unit time) from the Ambuklao reservoir with all eight spillway gates fully open and normal reservoir water level (NWL) at EL.752 m as shown in Fig.10.23.

The powerplant releases at $61.4 \text{ m}^3/\text{sec}$. for all three units operating at full gate opening were also considered.

(iii) Reservoir Water Level

The initial water level at the downstream end of the Binga reservoir was assumed to be at the L.W.L., or EL.555 m.

The water level was determined on the basis of the relation between the inflow and the amount of water required for power production ($88 \text{ m}^3/\text{sec}$ at L.W.L.).

When the water level exceeded the level of the spillway crest, EL.563 m, the corresponding reservoir water levels were determined by considering the water discharges through the spillway.

(iv) Grain Size Distribution

The grain size distribution of Sample Nos. 3, 5, 6, 8 and 9 shown in Fig.10.5 were used as representative of the respective reservoir bed sections.

(3) Conclusions

The sediments deposited in the upstream reaches of the Binga reservoir can be flushed out by large amount discharges through the Ambuklao spillway assuming that all eight spillway gates fully open and that at the start of the operation the Ambuklao reservoir water level will be kept at NWL (EL.752 m), while the Binga reservoir water level will be kept at L.W.L. (EL.555 m). Both reservoirs will be operated in the above manner until the Ambuklao reservoir water level is lowered to the spillway crest at EL.740 m.

The resultant decrease in the sediment level at the Ambuklao tailrace outlet would be 1.23 m. The decrease in the level of sediments would amount to 2.1 m, if the same spillway operation is repeated three times.

The total amount of water discharged through the spillway from the Ambuklao reservoir for this operation would be about $70 \times 10^6 \text{ m}^3$ for each sequence of operation.

10.3.2. Dredging of the Sediments along the Relevant River Course

This method was studied for the Ambuklao tailrace sedimentation problem, together with the method of the tailrace tunnel extension, in the Final Report of the Ambuklao Dam Rehabilitation Project prepared by JICA in March, 1988. As a result of the economic comparison of both methods, this method was adopted.

Prior to comparing the above dredging method with the method of removing the sediments by the Ambuklao reservoir operation as studied herein, the former method is outlined, from the above Final Report, as follows:

- 1) The relevant river course for dredging is proposed for a length of 1,500 m downstream of the outlet of the existing tailrace tunnel, with a gradient of the dredging channel to 1/1,130 or 1/1,675, dredging depth of 0.6 m to 1.0 m and dredging width of 25 m to 100 m. Eight different schemes were studied combining the above factors related to the dredging.
- 2) The increase in power generation was obtained by seeking a decrease in the tailrace outlet water level with non-uniform flow calculations applied to the above each scheme.
- 3) The quantities of dredging for each scheme were estimated.
- 4) In the result of the above procedure, the scheme which produces the maximum increase in power generation per unit amount of dredging was deemed as optimum.

The scheme adopted as above has the following features:

Optimum Scheme

- Gradient of dredging channel : 1/1,675
- Dredging depth at the outlet of tailrace tunnel: 1.0 m
- Dredging width : 25 m
- Quantities of dredging : 54,600 m³
- Tailrace outlet water level after dredging : EL.577.791 m
- Decrease in the tailrace outlet water level: 1.270 m
- Increase in power generation of the Ambuklao Plant: 0.88 %

The increase in power generation is found about 0.9 % against the decrease of 1.27 m in the tailrace outlet water level.

10.4. Sedimentation in the Reservoir and Its Influence on Power Generation

10.4.1. Change in Power Generation of the Binga Plant According to Progress of the Reservoir Sedimentation

Firstly, changes in annual power generation of the Binga Plant are calculated according to the progress of the reservoir sedimentation using the reservoir water level-storage capacity curve worked out on the basis of the future sedimentation anticipated, as referred to in the foregoing section 10.2.3, up to the year 2022. In general, once a pattern of the annual inflow to the reservoir be fixed, it is possible to calculate the annual power generation based on the reservoir water level - storage capacity curve following a certain rule of the reservoir operation. Hence, in case of changes in the effective storage volume of the reservoir, it is also possible to know a fluctuation of the annual power generation which is obtained using thus changed water level-storage capacity curve in obedience to the same rule of the reservoir operation.

As for Binga, the inflow to the reservoir is subjected to the flow control at the Ambuklao reservoir just upstream thereof,

under which situation the inflow to the Ambuklao reservoir is largely utilized for the power generation ($61.4 \text{ m}^3/\text{sec.}$). On the other hand, the Binga reservoir effective storage capacity is small as $39 \times 10^6 \text{ m}^3$ equivalent to five times the maximum daily water volume used for the power generation ($92 \text{ m}^3/\text{sec.}$) as of 1986, hence it is hard to get an effective answer in terms of power generation on a monthly basis.

In view of the above, the annual power generation of the Binga plant was sought on the basis of the annual inflow pattern in 1980 which was chosen as a typical pattern out of those in the last ten years from 1977 to 1986. It was calculated on a daily basis using the daily inflow consisting of the discharges from the tailrace and from the spillway associated with the Ambuklao Plant, and the inflow from the basin between the Ambuklao and Binga dams. Besides, the reservoir operation rule set the actual water volume used for the power generation as a target water volume applied to the calculation.

The result of the calculation is shown in the following table where the decrease in power generation affected by the decrease in the reservoir storage capacity due to sedimentation is not so noticeable, and it has turned out that the power generation in 2010 when the effective storage capacity would have come down to $26.5 \times 10^6 \text{ m}^3$ equivalent to 68% of 1986 indicated no more than minus 0.6 % compared with that in 1986. This reveals that the seasonal control of the river run-off is done at the Ambuklao reservoir having a large storage capacity, the Binga plant makes use of this controlled run-off from the Ambuklao just like a run-of-river type hydro powerstation and also that the Binga reservoir plays a role of adjusting the discharge on a weekly or daily basis. Hence, it is concluded that decrease in the effective storage capacity of the Binga reservoir due to sedimentation will give no serious influence on the annual power generation.

Progress of Sedimentation in the Reservoir and Annual Power Generation

<u>Year</u>	<u>Reservoir Storage Capacity (10^6 m^3)</u>			<u>Annual Generated Energy</u>	
	<u>Gross</u>	<u>Effective</u>	<u>(Ratio)</u>	<u>GWh</u>	<u>(Ratio)</u>
1986	61.5	39.0	(100)	481	(100)
1990	55.0	37.0	(95)	481	(100)
2000	41.5	32.0	(82)	480	(99.8)
2010	28.5	26.5	(68)	478	(99.4)

10.4.2. Loss and Increment of Generated Energy Incidental to Implementation of Measures against Sedimentation at the Upstream Reaches of the Reservoir

(1) Loss and Increment of Generated Energy Caused by Flushing out the Sediments

The method of flushing out the sediments is intended to recover the generation loss due to the raise of the river bed level at the Ambuklao tailrace outlet. To implement this method requires the Binga reservoir operation, thereby the power generation of the plant is surely affected so much.

Influence on the Ambuklao and the Binga plants given by the water discharge from the Ambuklao spillway for removal of the sediments is envisaged as follows:

For the Ambuklao Plant

- a) Loss of generated energy due to the dead discharge from the spillway

- b) Loss of generated energy due to drawdown of the reservoir water level by the discharge, that is loss of the head.
- c) Increment of generated energy owing to the recovery of the head made by removal of the sediments.

For the Binga Plant

- a) Loss of generated energy due to the dead discharge from the Ambuklao spillway.
- b) Loss of generated energy resultant from decrease of the effective storage capacity caused by the removal of sediments into the Binga reservoir.

The loss and increment of generated energy as mentioned above are calculated and shown in the following table. The total loss for both power plants induced by the method of flushing out the sediments amounts to 49.005 GWh and the total increment amounts to 3.031 GWh, which makes the balance 45.974 GWh of loss. This amount of loss corresponds to 5.5% of the total annual power generation of both power plants; $354.6 \text{ GWh} + 481.1 \text{ GWh} = 835.7 \text{ GWh}$.

Loss and Increment of Power Generation
Caused by Flushing out the Sediments

				(GWh)
	Cause of Loss/Increment	Loss	Increment	Total
Ambuklao Plant	Dead discharge from the spillway	27.607	-	Δ 27.607
	Loss of the head due to the dead discharge	1.231	-	Δ 1.231
	Gain of the head owing to flushing the sediments	-	3.031	+3.031
Sub-total		28.838	3.031	Δ 25.807
Binga Plant	Dead discharge from the Ambuklao spillway	20.167	-	Δ 20.167
	Decrease of the effective storage capacity of the reservoir	0	-	0
	Sub-total		20.167	-
Total		49.005	3.031	Δ 45.974

The conditions and method used for the above calculations are as below:

For the Ambuklao Plant

Main values used for the calculation are shown in the table below:

<u>Reservoir Water Level (EL.m)</u>	<u>Reservoir Storage Capacity (x10⁶ m³)</u>	<u>Utility Ratio (m³/kwh)</u>
752 (H.W.L.)	216.7	2.442
740 (Invert of spillway)	146.8	2.622
Difference/average	69.9	2.532

a) Loss of Power Generation due to the Dead Discharge (E1)

The discharge from the spillway is effected by full opening of the gates at H.W.L. of the Ambuklao reservoir and continued until the water level has reached L.W.L. The volume of such discharge was obtained from the water level-storage capacity curve and proved to be $69.9 \times 10^6 \text{ m}^3$.

The loss of power generation equivalent to the dead discharge proved to be 27.607 GWh with the formula $E1 = V/\eta$ applied giving $\eta = 2.532 \text{ m}^3/\text{KWh}$ for an average utility ratio between H.W.L. and L.W.L.

b) Loss of Power Generation due to Loss of the Head Resultant from Decrease in the Reservoir Water Level (E2)

- i) During the water level being decreased (during discharge)

Without the discharge, the plant is operable at H.W.L. However, decrease in the reservoir water level will reduce an efficiency of power generation. This reduction of efficiency corresponds to loss of the power generation. From the result of the hydraulic analysis on removal of the sediments as referred to in the foregoing 10.3.1, and assuming that transit time from H.W.L. to L.W.L. (T) would be 12 hours, the power generation expected at H.W.L. during the transit time (e1) is expressed;

$$e1 = (61.4 \text{ m}^3/\text{sec.} \times T \times 3600) / 2.442 = 1.086 \text{ GWh}$$

Then, the actual power generation during the transit time (e2) is expressed;

$$e2 = (61.4 \text{ m}^3/\text{sec.} \times T \times 3600) / 2.532 = 1.048 \text{ GWh}$$

Hence, loss of power generation ($\Delta 1$) is;

$$\Delta 1 = e1 - e2 = 0.038 \text{ GWh}$$

ii) During the water level being recovered

The discharge from the spillway to remove the sediments is to be effected in the month when the river run-off reaches the maximum. According to the inflow record of the Ambuklao reservoir for a period of 17 years from 1968 to 1984, the maximum monthly inflow is found in August with the average inflow of 304.63 MCM or $113.736 \text{ m}^3/\text{sec.}$

If the water level recovers up to H.W.L. in parallel with the operation of the Ambuklao Plant which requires water of $61.4 \text{ m}^3/\text{sec.}$, the time of recovery (T) is expressed;

$$T = 69.9 \times 10^6 / (113.736 - 61.4) / 3600 = 371.0 \text{ hrs.}$$

The power generation expected at H.W.L. during the recovery time (e1) is expressed;

$$e1 = (61.4 \text{ m}^3/\text{sec.} \times T \times 3600) / 2.442 = 33.581 \text{ GWh}$$

Then, the actual power generation during the recovery time (e2) is expressed;

$$e2 = (61.4 \text{ m}^3/\text{sec.} \times T \times 3600)/2.532 \\ = 32.388 \text{ GWh}$$

Hence, loss of power generation ($\Delta 2$) is;

$$\Delta 2 = e1 - e2 = 1.193 \text{ GWh}$$

Consequently, total loss of power generation due to decrease in the reservoir water level (E2) is expressed;

$$E2 = \Delta 1 + \Delta 2 = 0.038 + 1.193 = 1.231 \text{ GWh}$$

c) Increment of Power Generation Owing to Gain of the Head (E3)

According to the result of the hydraulic analysis on removal of the sediments as referred to in 10.3.1, a gain of the head attributable to flushing the sediments away at and around the outlet of the tailrace tunnel was found 1.23 m for one discharge. The increments of the plant output and annual power generation are shown as 0.695% and 354.56 GWh respectively in the Final Report of the Ambuklao Dam Rehabilitation Project of March, 1988.

From the above, the increment of power generation due to gain of the head (E3) is expressed;

$$E3 = 354.56 \text{ GWh} \times 0.695 \% \times 1.23 = 3.031 \text{ GWh}$$

For the Binga Plant

Main values used for the calculation are shown in the table below:

<u>Reservoir Water Level (EL.m)</u>	<u>Reservoir Storage Capacity ($\times 10^6 \text{ m}^3$)</u>	<u>Utility Ratio (m^3/KWh)</u>
575 (H.W.L.)	60.7	2.742
563 (Invert of spillway)	33.9	3.000
575 to 563 (Difference/average)	(26.8)	(2.871)
555 (L.W.L.)	21.9	3.202
563 to 555	12.0	

a) Loss of Power Generation due to the Dead Discharge (E1)

The discharge from the Ambuklao spillway is effected at the time the Binga reservoir water level stands at the lowest so as to expect the most effectiveness of removing the sediments downstream. Out of the discharge from the Ambuklao amounting to $69.9 \times 10^6 \text{ m}^3$, the Binga reservoir can accommodate $12 \times 10^6 \text{ m}^3$ which represents the possible storage capacity between EL.563 m on the invert of the spillway and EL.555 m, the lowest water level. Hence, the dead discharge from the Binga dam is $57.9 \times 10^6 \text{ m}^3$ ($69.9 - 12.0$), and the loss of power generation (E1) is expressed;

$$E1 = 57.9 \times 10^6 / 2.871 = 20.167 \text{ GWh}$$

b) Loss of Power Generation due to Decrease in the Binga Reservoir Storage Capacity

The analysis of the riverbed movement at the discharge for removing the sediments was carried out in the foregoing section 10.2.3. Taking the result of this analysis into account, the reservoir water level and storage capacity before and after the discharge in the year 1986 are correlated as shown in the following table as well as for 1990 just for comparison purpose.

Changes in Effective Storage Capacity of the Binga Reservoir due to Removal of Sediments

Reservoir Water Level (m)	1986		1990
	Before Discharge	After Discharge	
H.W.L. 575	60.83	58.33	55.00
L.W.L. 555	21.90	21.87	17.97
Effective Storage Capacity	38.93	36.46	37.03

($\times 10^6 \text{ m}^3$)

From the above table, it is found out that the effective storage capacity after the discharge for removing the sediments approximates to that estimated for 1990. Taking into consideration the outcome that there is no difference in the annual power generation between 1986 and 1990 caused by the progress of sedimentation as referred to in the foregoing section 10.4.1, a decrease in power generation due to the discharge, if any, can be ignored accordingly.

(2) Increment of Generated Energy Owing to Dredging

The proposed dredging is put into effect in the dry season

not to hamper the operation of both the Ambuklao and the Binga plants. Since this method involves neither a dead discharge nor a drawdown of the reservoir water level, no loss of power generation is caused at all. The increment of power generation is shown in the Final Report of the Ambuklao Dam Rehabilitation Project and is summarized as below:

$$354.56 \text{ GWh} \times 0.88 \% = 3.120 \text{ GWh}$$

11. PROPOSED REHABILITATION PROGRAM

11. Proposed Rehabilitation Program

11.1. Rehabilitation Schemes

The proposed Binga dam rehabilitation Project consists of the following three schemes:

- Dam Upstream Face Rehabilitation Scheme
- Dam Toe Protection Retaining Wall Rehabilitation Scheme
- Left Bank Excavated Slope Rehabilitation Scheme

As the result of the initial field survey conducted by the JICA study team, erosion on the foundation concrete at the downward end of the spillway apron had been found in progress to such a level that it requires some repairs. In this connection, NAPOCOR has already finished the definite design, and is currently in the process of selecting a contractor for the repair works. Hence, this repair scheme was not included here.

The details of the above each scheme are described below:

11.1.1. Dam Upstream Face Rehabilitation Scheme

The cross-sectional survey of the dam embankment was conducted to study the stability. Comparison of the actual current cross section of the dam with that at the completion of the dam reveals that the former has been reduced, particularly for the section of the upstream upper slope of the dam corresponding to EL.557 m to EL.586 m. (The current slope is 1:1.30 while the as-built slope was 1:1.35.)

As the result of the analysis on the current dam stability against sliding in both cases of the normal condition and the earthquake effects included with the reservoir water level varied among FWL, NWL and LWL, it turned out that no problem of

the stability would be caused at the normal condition, but the safety factor against sliding with regard to the small slide at the upstream upper slope shows a value below 1.0 in the case of the earthquake effects included at FWL.

In view of the above, it is proposed to fill rock materials on the current upstream face slope between EL. 557 m and EL. 586 m in order to increase the dam stability at the earthquake as well as to reinstate the slope damaged by wind and wave actions. The gradient of the rock-filled slope as remedied above shall be designed to be 1:2.23 so that the safety factor against sliding at the earthquake may reach above 1.0 as mentioned in the foregoing section 7. Besides, the rock size for the slope protection was calculated with the Hudson formula as shown below, thereby it proved to be 0.8 m in diameter (weight: 0.7 ton).

Hudson Formula

$$W = \frac{W_r \cdot H^3}{K_D (W_r/W_o - 1)^3 \text{Cot } \alpha}$$

Where,

- W : Weight of rock (ton)
- W_r : Unit weight of rock (2.6 ton/m³)
- W_o : Unit weight of water (1.0 ton/m³)
- α : Angle of slope against horizontal plane
(Cot α=2.23)
- H : Wave height (1.7 m at fetch length of 1.4 km,
wind velocity of 50 m/sec.)
- K_D : Constant 2 (2-5)

With the above conditions applied, W=0.699 ton and D=0.801 m are obtained accordingly.

The quantities of the proposed rock filling can be obtained from the difference between the design cross section of the dam and the actual measured section, thus showing 50,500 m³.

As a conclusion, this scheme is summarized as follows:

- (a) Area of Rock-filling : EL.557 m to EL.586 m
- (b) Finished slope gradient : 1 : 2.23
- (c) Rock materials : 0.8 m in diameter (W:700 kg)
- (d) Design quantities of rock materials: 50,500 m³

11.1.2. Dam Toe Protection Retaining Wall Rehabilitation Scheme

The toe of the dam downstream slope lies near to the plunge pool into which the discharge from the spillway chute is plunged, thereby causing the whirl water flow. With this situation, the large discharge may possibly scour the toe portion of the dam downstream slope. For this reason, the concrete retaining wall was constructed to protect the toe portion after completion of the dam. However, the wall was scoured with its foundation and heavily damaged during the big flood that occurred in June, 1976 equivalent to the maximum flood inflow of 2,602 m³/sec. The wall was not repaired after the incident. Since June, 1976, no big floods as above have ever occurred to date, thus the toe portion of the dam has been prevented from scouring. In view of the dam safety control, however, the damaged wall should be urgently rehabilitated.

In accordance with the original design drawings, the wall was 92 meters long and its top was at EL.496 meters. It was designed to accommodate a flood with a water level at 494.0 meters. Presently, the wall is separated into three portions. Approximately one third of the wall towards the left abutment (spillway) has remained as originally constructed and is situated on the bedrock, the one third middle portion is

inclined about 20° downstream and the remaining one third toward the right abutment is as well inclined some 45°.

As measures for the rehabilitation of the wall, two schemes are considered, one is to construct a concrete wall of a similar design in replacement of the current damaged wall and the other is to provide a rock dyke composed of appropriate size rock particles.

The drilling investigations carried out at three locations along the existing wall have indicated that bedrocks at these locations were at EL.485.7 m, EL.466.7 m and EL.465.7 m from the left bank side.

The results of the hydraulic studies for the plunge pool have shown that the water level of the plunge pool would rise to EL.500 m if the discharge of 6,600 m³/sec. from the spillway is made at the normal maximum reservoir water level of EL.575 m.

Hence, in view of the above, a rather deep excavation will have to be made in order to reach the bedrock for construction of the wall, thus, resulting in a huge structure as tall as about 35 m. Further, a self-support type concrete wall was also considered since the foundation need not reach the bedrock. However, once it has turned over, it would be very difficult to rehabilitate as required.

Taking all the above into account, it is concluded that the rock dyke scheme is the most suitable for the rehabilitation of the wall. The advantage of this, is that, the existing damaged wall can be used, as it is, as a part of the rock dyke and that rock materials are available in the nearby dam site. In addition, the rock dyke has superiority in the following aspects:

- The progress of scouring can be prevented by the rocks rolling down to fill the scoured part on the toe of the dyke since the rock dyke is abundant in flexibility as compared with the concrete structures.
- Scouring of the dyke can be well prevented by using rock materials with an appropriate grading of rock sizes.

From the results of the topographic survey at the toe of the dam downstream slope and the hydraulic analysis on the plunge pool, the main design characteristics of the proposed rock dyke are determined as follows:

Main Design Characteristics of the Rock Dyke

Type	: Dumped rockfill type
Gradient	: EL.502 m to EL.493 m; 1 : 5.5 EL.493 m to bottom level; 1 : 2 (+EL.485 m)
Grading of rock sizes	: Mean diameter; 0.5 m (weight = 200 kg)
Riprap material	: Max. 1.0 m in diameter (weight = 1.3 ton)
Quantities of rock materials	: 15,000 m ³

11.1.3. Left Bank Excavated Slope Rehabilitation Scheme

The open-cut slope was formed after excavating approximately 360 million cubic meters across the mountain ridge projecting from the left bank in order to construct the spillway. The excavated debris was used for embankment materials of the dam.

The excavated slope presents a triangular appearance of 130 m high and 500 m long at the bottom, and consists of seven berms of 8.5 m wide and 20 m high each. The average slope of the cut is approximately 60°.

From the geological point of view, this excavated slope consists of metamorphic rocks which had originated from andesitic and basaltic lava, and sedimentary rocks, such as tuff and tuff breccia.

The stability analysis conducted for the excavated slope of the spillway open cut excavation based on the actual profile prepared this time has indicated that the slope is stable and safe against sliding, as shown in the foregoing section 8.

The slope as originally excavated was not provided with any surface protection, as, apparently, at the time of construction, and during the period of 30 years since its completion, more than 10 points of the slope have been subjected to damages and local failures mainly due to erosion by rainfall. However, as mentioned above, the slope as a whole has not been affected, since most of the rocks where the slope is formed, are hard and in a stable condition.

Consequently, it is proposed for the repair works of the excavated slope to remove the debris remained on the berms and also to prevent further progress of erosion on the slope surface by rainfall. For implementing the above proposal, a shotcreting method is recommended for the following reason:

- To be superior in shutting out air and rainfall which has a big effect to prevent the slope from weathering.
- Shotcreting machines of a simple and small movable type are suitable for an operation at narrow and high places like this open-cut slope.
- The difference in temperature throughout the year is not remarkable, thus, there is no fear of freezing.

The damages and local failures of the slope which need shotcreting are located in fifteen different points as shown in Fig.11.7.

The major design characteristics of shotcreting are as follows:

Design Characteristics of Shotcreting

- (1) Kind of shotcreting : Concrete spraying
- (2) Thickness finished : 15 cm
- (3) Mesh size : 50 mm - 100 mm
- (4) Reinforcing bars : 10 mm in diameter,
50 cm interval grid
- (5) Anchor pins : 16 mm in diameter,
1 m long, 0.5 pcs./m²
- (6) Place of shotcreting : 15 points
- (7) Area of shotcreting : 13,000 m²

11.2. Implementation Program

11.2.1. Dam Upstream Face Rehabilitation Scheme

A quarry site of rock materials is proposed at the left bank upstream of the ex-quarry site of the existing dam. In this connection, the detail geological investigations including drilling, seismic prospecting, test of rock materials and so forth should be carried out before implementation of the proposed scheme.

The scheme will be put into effect initiated by pre-operation arrangements of the proposed quarry, which include temporary facilities, clearing, stripping, benching and hauling road. This arrangements will take five months. Beside, it is required to rehabilitate the old approach road to the ex-quarry site which was located along the right bank upstream of the dam.

This can be achieved when the reservoir water level gets down to L.W.L.

Collection of the rock materials will be effected by the short bench cut method using a crawler drill. Heaping up and loading of rocks are done with a 32 ton class bulldozer and a tractor shovel of 3 m³ capacity, respectively, and hauling of rocks is done by a 11 ton class dump truck in view of the road condition.

The rock materials are hauled through the approach road on the right bank of the dam to the point of filling. Thereafter, those shall be placed uniformly and compacted by a 32 ton class bulldozer starting at EL.555 m.

The irregularities and unsuitable materials on the existing surface of the rockfills shall be eliminated by a back-hoe of 1 m³ capacity or manpower prior to the proposed rock filling. The surface finish of the rock filling shall be made by either a back-hoe or a 11 ton class truck crane, following the completion of the rock filling.

The top soil and debris stemmed from the quarry operation shall be spoiled at the flat area on the right bank downstream of the dam which is used as a spoil bank. The spoil bank shall be formed properly by a bulldozer and back-hoe.

The whole period of the proposed 50,500 m³ rock filling works at the dam upstream slope is estimated about twelve (12) months. However, this period is based on the condition that the filling works could be finished in one dry season, and the reservoir water level be kept as low as EL.555 m throughout the working period.

The above schedule is illustrated in Table 11.1.

11.2.2. Dam Toe Protection Retaining Wall Scheme

The rock materials shall be available from the same quarry as used for the rock filling on the dam upstream face slope mentioned in (1) above. The rock materials collected by the short bench cut method are bulldozed down along the bench slope by a 31 ton class bulldozer, thereafter shall be subject to an appropriate grading of rock sizes. The coarse rock materials selected for the filling material shall be used for the proposed construction work.

The proposed construction of a rock dyke shall be commenced with mobilization of the construction equipment through the access road located on the right bank of the dam downstream. The construction equipment consists of a 31 ton class bulldozer and a back-hoe of 1 m³ capacity. Using these equipment, the riverbed which forms a foundation of the proposed rock dyke shall be rearranged and cleared of any unsuitable materials, following which treatment, void portions under the collapsed retaining wall shall be filled with rock materials. Subsequently, filling for the rock dyke shall be commenced from the downstream end of the dam.

Collection, hauling and filling of the rock materials, and surface finish of the filling shall follow the same method as applied to the rock filling on the dam upstream face slope. The debris stemmed from the quarry operation shall be spoiled at a specified spoil bank as well.

The whole period of the proposed 15,000 m³ rock filling works at the dam downstream slope is estimated approximately seven (7) months. However, this period is based on the condition that the filling works could be finished in a dry season and the discharge from the dam is minimal.

The above schedule is illustrated in Table 11.1.

11.2.3. Left Bank Excavated Slope Rehabilitation Scheme

(1) Removal of Debris

The proposed repair works shall be set about just after completion of the quarry operation on the left bank. An access road to each berm of the excavated slope from the upstream end of the proposed quarry site shall be improved properly. The debris deposited on the berm which stemmed from local failure of the open-cut slope shall be removed from the berm starting from the higher elevation. The debris shall be scraped off by manpower and a small back-hoe, then shall be loaded on a 8 ton dump truck by a small tractor shovel and hauled out.

The collapsed portion of the berm shall be provided with a temporary pier to enable passage of a small shovel machine or the like.

(2) Shotcreting

Subsequent to the removal of the debris as mentioned in (3) above, shotcreting shall be commenced to protect the slope. It shall be effected from higher portions to lower portions, starting with eliminating rocks on the slope which are about to fall, followed by fixing wire nets on the relevant area of the slope.

The sprayer with a capacity of 5 m³ per hour shall be used for shotcreting. The fine aggregate to be used for the shotcrete materials shall be purchased and delivered to the site. The stock facilities of the fine aggregate shall be provided at the site as well as those of cement.